

# Event Shape/Energy Flow Correlations

**Carola F. Berger, Tibor Kúcs, and George Sterman**

*C.N. Yang Institute for Theoretical Physics, Stony Brook University, SUNY  
Stony Brook, New York 11794 – 3840, U.S.A.*

## Abstract

We introduce a set of correlations between energy flow and event shapes that are sensitive to the flow of color at short distances in jet events. These correlations are formulated for a general set of event shapes, which includes jet broadening and thrust as special cases. We illustrate the method for  $e^+e^-$  dijet events, and calculate the correlation at leading logarithm in the energy flow and at next-to-leading-logarithm in the event shape.

## 1 Introduction

The agreement of theoretical predictions with experiment for jet cross sections is often impressive. This is especially so for inclusive jet cross sections at high  $p_T$ , using fixed-order factorized perturbation theory and parton distribution functions [1]. A good deal is also known about the substructure of jets, through the theoretical and experimental study of multiplicity distributions and fragmentation functions [2], and of event shapes [3, 4, 5]. Event shape distributions [6, 7, 8] in particular offer a bridge between the perturbative, short-distance and the nonperturbative, long-distance dynamics of QCD [9].

Energy flow [10] into angular regions between energetic jets gives information that is in some ways complementary to what we learn from event shapes. In perturbation theory, the distribution

of particles in the final state reflects interference between radiation from different jets [2], and there is ample evidence for perturbative antenna patterns in interjet radiation at both  $e^+e^-$  [11] and hadron colliders [12, 13]. Energy flow between jets must also encode the mechanisms that neutralize color in the hadronization process, and the transition of QCD from weak to strong coupling. Knowledge of the interplay between energy and color flows [14, 15] may help identify the underlying event in hadron collisions [16], to distinguish QCD bremsstrahlung from signals of new physics. Nevertheless, the systematic computation of energy flow into interjet regions has turned out to be subtle [17] for reasons that we will review below, and requires a careful construction of the class of jet events. It is the purpose of this work to provide such a construction, using event shapes as a tool.

In this paper, we introduce correlations between event shapes and energy flow, “shape/flow correlations”, that are sensitive primarily to radiation from the highest-energy jets. So long as the observed energy is not too small, in a manner to be quantified below, we may control logarithms of the ratio of energy flow to jet energy [15, 18].

The energy flow observables that we discuss below are distributions associated with radiation into a chosen interjet angular region,  $\Omega$ . Within  $\Omega$  we identify a kinematic quantity  $Q_\Omega \equiv \varepsilon Q$ , at c.m. energy  $Q$ , with  $\varepsilon \ll 1$ .  $Q_\Omega$  may be the sum of energies, transverse energies or related observables for the particles emitted into  $\Omega$ . Let us denote by  $\bar{\Omega}$  the complement of  $\Omega$ . We are interested in the distribution of  $Q_\Omega$  for events with a fixed number of jets in  $\bar{\Omega}$ . This set of events may be represented schematically as

$$A + B \rightarrow \text{Jets} + X_{\bar{\Omega}} + R_\Omega(Q_\Omega). \quad (1)$$

Here  $X_{\bar{\Omega}}$  stands for radiation into the regions between  $\Omega$  and the jet axes, and  $R_\Omega$  for radiation into  $\Omega$ .

The subtlety associated with the computation of energy flow concerns the origin of logarithms, and is illustrated by Fig. 1. Gluon 1 in Fig. 1 is an example of a primary gluon, emitted directly from the hard partons near a jet axes. Phase space integrals for primary emissions contribute single logarithms per loop:  $(1/Q_\Omega)\alpha_s^n \ln^{n-1}(Q/Q_\Omega) = (1/\varepsilon Q)\alpha_s^n \ln^{n-1}(1/\varepsilon)$ ,  $n \geq 1$ , and these logarithms exponentiate in a straightforward fashion [15]. At fixed  $Q_\Omega$  for Eq. (1), however, there is another source of potentially large logarithmic corrections in  $Q_\Omega$ . These are illustrated by gluon 2 in the figure, an example of secondary radiation in  $\Omega$ , originating a parton emitted by one of the leading jets that define the event into intermediate region  $\bar{\Omega}$ . As observed by Dasgupta and Salam [17], emissions into  $\Omega$  from such secondary partons can also result in logarithmic corrections, of the form  $(1/Q_\Omega)\alpha_s^n \ln^{n-1}(\bar{Q}_{\bar{\Omega}}/Q_\Omega)$ ,  $n \geq 2$ , where  $\bar{Q}_{\bar{\Omega}}$  is the maximum energy emitted into  $\bar{\Omega}$ . These logarithms arise from strong ordering in the energies of the primary and secondary radiation because real and virtual enhancements associated with secondary emissions do not cancel each other fully at fixed  $Q_\Omega$ .

If the cross section is fully inclusive outside of  $\Omega$ , so that no restriction is placed on the radiation into  $\bar{\Omega}$ ,  $\bar{Q}_{\bar{\Omega}}$  can approach  $Q$ , and the secondary logarithms can become as important as the primary logarithms. Such a cross section, in which only radiation into a fixed portion of phase space ( $\Omega$ ) is specified, was termed “non-global” by Dasgupta and Salam, and the associated logarithms are also called non-global [17, 19, 20].

In effect, a non-global definition of energy flow is not restrictive enough to limit final states to a specific set of jets, and non-global logarithms are produced by jets of intermediate energy, emitted in directions between region  $\Omega$  and the leading jets. Thus, interjet energy flow does not always originate directly from the leading jets, in the absence of a systematic criterion for suppressing intermediate radiation. Correspondingly, non-global logarithms reflect color flow at all scales, and do not exponentiate in a simple manner. Our aim in this paper is to formulate a set of observables for interjet radiation in which non-global logarithms are replaced by calculable corrections, and which reflect the flow of color at short distances. By restricting the sizes of event shapes, we will limit radiation in region  $\bar{\Omega}$ , while retaining the chosen jet structure.

An important observation that we will employ below is that non-global logarithms are not produced by secondary emissions that are very close to a jet direction, because a jet of parallel-moving particles emits soft radiation coherently. By fixing the value of an event shape near the limit of narrow jets, we avoid final states with large energies in  $\bar{\Omega}$  away from the jet axes. At the same time, we will identify limits in which non-global logarithms reemerge as leading corrections, and where the methods introduced to study nonglobal effects in Refs. [17, 19, 20] provide important insights.

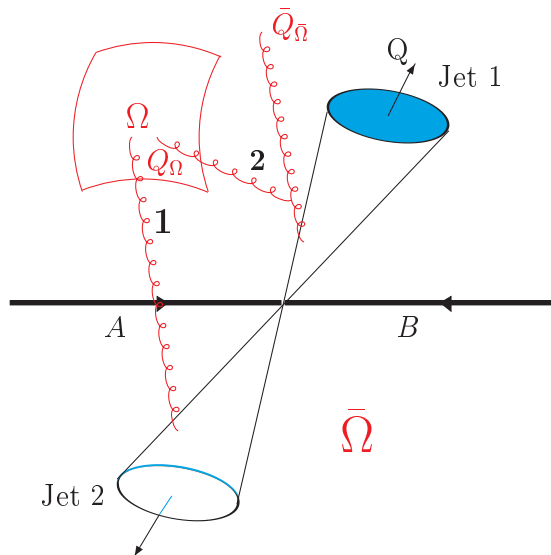


Figure 1: Sources of global and non-global logarithms in dijet events. Configuration 1, a primary emission, is the source of global logarithms. Configuration 2 can give non-global logarithms.

To formalize these observations, we study below correlated observables for  $e^+e^-$  annihilation into two jets. (In Eq. (1)  $A$  and  $B$  denote positron and electron.) In  $e^+e^-$  annihilation dijet events, the underlying color flow pattern is simple, which enables us to concentrate on the energy flow within the event. We will introduce a class of event shapes,  $\bar{f}(a)$  suitable for measuring energy flow into only part of phase space, with  $a$  an adjustable parameter. To avoid large

non-global logarithmic corrections we weight events by  $\exp[-\nu\bar{f}]$ , with  $\nu$  the Laplace transform conjugate variable.

For the restricted set of events with narrow jets, energy flow is proportional to the lowest-order cross section for gluon radiation into the selected region. The resummed cross section, however, remains sensitive to color flow at short distances through anomalous dimensions associated with coherent interjet soft emission. In a sense, our results show that an appropriate selection of jet events automatically suppresses nonglobal logarithms, and confirms the observation of coherence in interjet radiation [2, 12].

In the next section, we introduce the event shapes that we will correlate with energy flow, and describe their relation to the thrust and jet broadening. Section 3 contains the details of the factorization procedure that characterizes the cross section in the two-jet limit. This is followed in Sec. 4 by a derivation of the resummation of logarithms of the event shape and energy flow, following the method introduced by Collins and Soper [21]. We then go on in Sec. 5 to exhibit analytic results at leading logarithmic accuracy in  $Q_\Omega/Q$  and next-to-leading logarithm in the event shape. Section 6 contains representative numerical results. We conclude with a summary and a brief outlook on further applications.

## 2 Shape/Flow Correlations

### 2.1 Weights and energy flow in dijet events

In the notation of Eq. (1), we will study an event shape distribution for the process

$$e^+ + e^- \rightarrow J_1(p_{J_1}) + J_2(p_{J_2}) + X_{\bar{\Omega}}(\bar{f}) + R_\Omega(Q_\Omega), \quad (2)$$

at c.m. energy  $Q \gg Q_\Omega \gg \Lambda_{\text{QCD}}$ . Two jets with momenta  $p_{J_c}$ ,  $c = 1, 2$  emit soft radiation (only) at wide angles. Again,  $\Omega$  is a region between the jets to be specified below, where the total energy or the transverse energy  $Q_\Omega$  of the soft radiation is measured, and  $\bar{\Omega}$  denotes the remaining phase space (see Fig. 1). Radiation into  $\bar{\Omega}$  is constrained by event shape  $\bar{f}$ . We refer to cross sections at fixed values (or transforms) of  $\bar{f}$  and  $Q_\Omega$  as shape/flow correlations.

To impose the two-jet condition on the states of Eq. (2) we choose weights that suppress states with substantial radiation into  $\bar{\Omega}$  away from the jet axes. We now introduce a class of event shapes  $\bar{f}$ , related to the thrust, that enforce the two-jet condition in a natural way.

These event shapes interpolate between and extend the familiar thrust [4] and jet broadening [7, 8], through an adjustable parameter  $a$ . For each state  $N$  that defines process (2), we separate  $\bar{\Omega}$  into two regions,  $\bar{\Omega}_c$ ,  $c = 1, 2$ , containing jet axes,  $\hat{n}_c(N)$ . To be specific, we let  $\bar{\Omega}_1$  and  $\bar{\Omega}_2$  be two hemispheres that cover the entire space except for their intersections with region  $\Omega$ . Region  $\bar{\Omega}_1$  is centered on  $\hat{n}_1$ , and  $\bar{\Omega}_2$  is the opposite hemisphere. We will specify the method that determines the jet axes  $\hat{n}_1$  and  $\hat{n}_2$  momentarily. To identify a meaningful jet, of course, the total energy within  $\bar{\Omega}_1$  should be a large fraction of the available energy, of the order of  $Q/2$  in dijet events. In  $e^+e^-$  annihilation, if there is a well-collimated jet in  $\bar{\Omega}_1$  with nearly half the total energy, there will automatically be one in  $\bar{\Omega}_2$ .

We are now ready to define the contribution from particles in region  $\bar{\Omega}_c$  to the  $a$ -dependent event shape,

$$\bar{f}_{\bar{\Omega}_c}(N, a) = \frac{1}{\sqrt{s}} \sum_{\hat{n}_i \in \bar{\Omega}_c} k_{i,\perp}^a \omega_i^{1-a} (1 - \hat{n}_i \cdot \hat{n}_c)^{1-a}, \quad (3)$$

where  $a$  is any real number less than two, and where  $\sqrt{s} = Q$  is the c.m. energy. The sum is over those particles of state  $N$  with direction  $\hat{n}_i$  that flow into  $\bar{\Omega}_c$ , and their transverse momenta  $k_{i,\perp}$  are measured relative to  $\hat{n}_c$ . The jet axis  $\hat{n}_1$  for jet 1 is identified as that axis that minimizes the specific thrust-related quantity  $\bar{f}_{\bar{\Omega}_1}(N, a = 0)$ . When  $\bar{\Omega}_c$  in Eq. (3) is extended to all of phase space, the case  $a = 0$  is then essentially  $1 - T$ , with  $T$  the thrust, while  $a = 1$  is related to the jet broadening.

Any choice  $a < 2$  in (3) specifies an infrared safe event shape variable, because the contribution of any particle  $i$  to the event shape behaves as  $\theta_i^{2-a}$  in the collinear limit,  $\theta_i = \cos^{-1}(\hat{n}_i \cdot \hat{n}_c) \rightarrow 0$ . Negative values of  $a$  are clearly permissible, and the limit  $a \rightarrow -\infty$  corresponds to the total cross section. At the other limit, the factorization and resummation techniques that we discuss below will apply only to  $a < 1$ . For  $a > 1$ , contributions to the event shape (3) from energetic particles near the jet axis are generically larger than contributions from soft, wide-angle radiation, or equal for  $a = 1$ . When this is the case, the analysis that we present below must be modified, at least beyond the level of leading logarithm [8].

In summary, once  $\hat{n}_1$  is fixed, we have divided the phase space into three regions:

- Region  $\Omega$ , in which we measure, for example, the energy flow,
- Region  $\bar{\Omega}_1$ , the entire hemisphere centered on  $\hat{n}_1$ , that is, around jet 1, except its intersection with  $\Omega$ ,
- Region  $\bar{\Omega}_2$ , the complementary hemisphere, except its intersection with  $\Omega$ .

In these terms, we define the complete event shape variable  $\bar{f}(N, a)$  by

$$\bar{f}(N, a) = \bar{f}_{\bar{\Omega}_1}(N, a) + \bar{f}_{\bar{\Omega}_2}(N, a), \quad (4)$$

with  $\bar{f}_{\bar{\Omega}_c}$ ,  $c = 1, 2$  given by (3) in terms of the axes  $\hat{n}_1$  of jet 1 and  $\hat{n}_2$  of jet 2. We will study the correlations of this set of event shapes with the energy flow into  $\Omega$ , denoted as

$$f(N) = \frac{1}{\sqrt{s}} \sum_{\hat{n}_i \in \Omega} \omega_i. \quad (5)$$

The differential cross section for such dijet events at fixed values of  $\bar{f}$  and  $f$  is now

$$\begin{aligned} \frac{d\bar{\sigma}(\varepsilon, \bar{\varepsilon}, s, a)}{d\varepsilon d\bar{\varepsilon} d\hat{n}_1} &= \frac{1}{2s} \sum_N |M(N)|^2 (2\pi)^4 \delta^4(p_I - p_N) \\ &\quad \times \delta(\varepsilon - f(N)) \delta(\bar{\varepsilon} - \bar{f}(N, a)) \delta^2(\hat{n}_1 - \hat{n}(N)), \end{aligned} \quad (6)$$

where we sum over all final states  $N$  that contribute to the weighted event, and where  $M(N)$  denotes the corresponding amplitude for  $e^+e^- \rightarrow N$ . The total momentum is  $p_I$ , with  $p_I^2 = s \equiv$

$Q^2$ . As mentioned in the introduction, for much of our analysis, we will work with the Laplace transform of (6),

$$\begin{aligned} \frac{d\sigma(\varepsilon, \nu, s, a)}{d\varepsilon d\hat{n}_1} &= \int_0^\infty d\bar{\varepsilon} e^{-\nu\bar{\varepsilon}} \frac{d\bar{\sigma}(\varepsilon, \bar{\varepsilon}, s, a)}{d\varepsilon d\bar{\varepsilon} d\hat{n}_1} \\ &= \frac{1}{2s} \sum_N |M(N)|^2 e^{-\nu\bar{f}(N,a)} (2\pi)^4 \delta^4(p_I - p_N) \\ &\quad \times \delta(\varepsilon - f(N)) \delta^2(\hat{n}_1 - \hat{n}(N)). \end{aligned} \quad (7)$$

Singularities of the form  $(1/\bar{\varepsilon}) \ln^n(1/\bar{\varepsilon})$  in the cross section (6) give rise to logarithms  $\ln^{n+1} \nu$  in the transform (7).

Since we are investigating energy flow in two-jet cross sections, we fix the constants  $\varepsilon$  and  $\bar{\varepsilon}$  to be both much less than unity:

$$0 < \varepsilon, \bar{\varepsilon} \ll 1. \quad (8)$$

We refer to this as the elastic limit for the two jets. In the elastic limit, the dependence of the directions of the jet axes on soft radiation is weak. We will return to this dependence below. Independent of soft radiation, we can always choose our coordinate system such that the transverse momentum of jet 1 is zero,

$$p_{J_1, \perp} = 0, \quad (9)$$

with  $\vec{p}_{J_1}$  in the  $x_3$  direction. In the limit  $\bar{\varepsilon}, \varepsilon \rightarrow 0$ , and in the overall c.m.,  $p_{J_1}$  and  $p_{J_2}$  then approach light-like vectors in the plus and minus directions:

$$\begin{aligned} p_{J_1}^\mu &\rightarrow \left( \sqrt{\frac{s}{2}}, 0^-, 0_\perp \right) \\ p_{J_2}^\mu &\rightarrow \left( 0^+, \sqrt{\frac{s}{2}}, 0_\perp \right). \end{aligned} \quad (10)$$

As usual, it is convenient to work in light-cone coordinates,  $p^\mu = (p^+, p^-, p_\perp)$ , which we normalize as  $p^\pm = (1/\sqrt{2})(p^0 \pm p^3)$ . For small  $\varepsilon$  and  $\bar{\varepsilon}$ , the cross section (6) has corrections in  $\ln(1/\varepsilon)$  and  $\ln(1/\bar{\varepsilon})$ , which we will organize in the following.

## 2.2 Weight functions and jet shapes

In Eq. (3),  $a$  is a parameter that allows us to study various event shapes within the same formalism; it helps to control the approach to the two-jet limit. As noted above,  $a < 2$  for infrared safety, although the factorization that we will discuss below applies beyond leading logarithm only to  $1 > a > -\infty$ . A similar weight function with a non-integer power has been discussed in a related context for  $2 > a > 1$  in [22]. To see how the parameter  $a$  affects the shape of the jets, let us reexpress the weight function for jet 1 as

$$\bar{f}_{\bar{\Omega}_1}(N, a) = \frac{1}{\sqrt{s}} \sum_{\hat{n}_i \in \bar{\Omega}_1} \omega_i \sin^a \theta_i (1 - \cos \theta_i)^{1-a}, \quad (11)$$

where  $\theta_i$  is the angle of the momentum of final state particle  $i$  with respect to jet axis  $\hat{n}_1$ . As  $a \rightarrow 2$  the weight vanishes only very slowly for  $\theta_i \rightarrow 0$ , and at fixed  $\bar{f}_{\bar{\Omega}_1}$ , the jet becomes very narrow. On the other hand, as  $a \rightarrow -\infty$ , the event shape vanishes more and more rapidly in the forward direction, and the cross section at fixed  $\bar{f}_{\bar{\Omega}_1}$  becomes more and more inclusive in the radiation into  $\bar{\Omega}_1$ .

In this paper, as in Ref. [15], we seek to control corrections in the single-logarithmic variable  $\alpha_s(Q) \ln(1/\varepsilon)$ , with  $\varepsilon = Q_\Omega/Q$ . Such a resummation is most relevant when

$$\alpha_s(Q) \ln\left(\frac{1}{\varepsilon}\right) \geq 1 \rightarrow \varepsilon \leq \exp\left(\frac{-1}{\alpha_s(Q)}\right). \quad (12)$$

Let us compare these logarithms to non-global effects in shape/flow correlations. At  $\nu = 0$  and for  $a \rightarrow -\infty$ , the cross section becomes inclusive outside  $\Omega$ . As we show below, the non-global logarithms discussed in Refs. [15, 17] appear in shape/flow correlations as logarithms of the form  $\alpha_s(Q) \ln(1/(\varepsilon\nu))$ , with  $\nu$  the moment variable conjugate to the event shape. To treat these logarithms as subleading for small  $\varepsilon$  and (relatively) large  $\nu$ , we require that

$$\alpha_s(Q) \ln\left(\frac{1}{\varepsilon\nu}\right) < 1 \rightarrow \varepsilon > \frac{1}{\nu} \exp\left(\frac{-1}{\alpha_s(Q)}\right). \quad (13)$$

For large  $\nu$ , there is a substantial range of  $\varepsilon$  in which both (12) and (13) can hold. When  $\nu$  is large, moments of the correlation are dominated precisely by events with strongly two-jet energy flows, which is the natural set of events in which to study the influence of color flow on interjet radiation. (The peak of the thrust cross section is at  $(1-T)$  of order one-tenth at LEP energies, corresponding to  $\nu$  of order ten, so the requirement of large  $\nu$  is not overly restrictive.) In the next subsection, we show how the logarithms of  $(\varepsilon\nu)^{-1}$  emerge in a low order example. This analysis also assumes that  $a$  is not large in absolute value. The event shape at fixed angle decreases exponentially with  $a$ , and we shall see that higher-order corrections can be proportional to  $a$ . We always treat  $\ln \nu$  as much larger than  $|a|$ .

### 2.3 Low order example

In this section, we check the general ideas developed above with the concrete example of a two-loop cross section for the process (2). This is the lowest order in which a non-global logarithm occurs, as observed in [17]. We normalize this cross section to the Born cross section for inclusive dijet production. A similar analysis for the same geometry has been carried out in [17] and [23].

The kinematic configuration we consider is shown in Fig. 2. Two fast partons, of velocities  $\vec{\beta}_1$  and  $\vec{\beta}_2$ , are treated in eikonal approximation. In addition, gluons are emitted into the final state. A soft gluon with momentum  $k$  is radiated into region  $\Omega$  and an energetic gluon with momentum  $l$  is emitted into the region  $\bar{\Omega}$ . We consider the cross section at fixed energy,  $\omega_k \equiv \varepsilon\sqrt{s}$ . As indicated above, non-global logarithms arise from strong ordering of the energies of the gluons, which we choose as  $\omega_l \gg \omega_k$ . In this region, the gluon  $l$  plays the role of a “primary” emission, while  $k$  is a “secondary” emission.

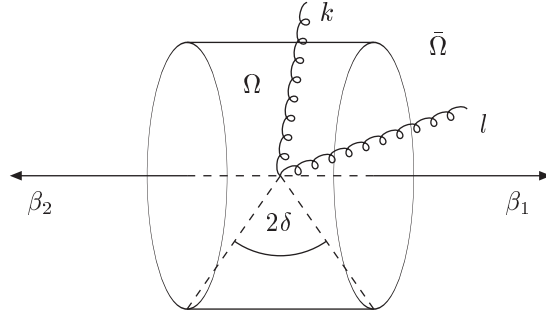


Figure 2: A kinematic configuration that gives rise to the non-global logarithms. A soft gluon with momentum  $k$  is radiated into the region  $\Omega$ , and an energetic gluon with momentum  $l$  is radiated into  $\bar{\Omega}$ . Four-vectors  $\beta_1$  and  $\beta_2$ , define the directions of jet 1 and jet 2, respectively.

For our calculation, we take the angular region  $\Omega$  to be a “slice” or “ring” in polar angle of width  $2\delta$ , or equivalently, (pseudo) rapidity interval  $(-\eta, \eta)$ , with

$$\Delta\eta = 2\eta = \ln \left( \frac{1 + \sin \delta}{1 - \sin \delta} \right), \quad (14)$$

The lowest-order diagrams for this process are those shown in Fig. 3, including distinguishable diagrams in which the momenta  $k$  and  $l$  are interchanged.

The diagrams of Fig. 3 give rise to color structures  $C_F^2$  and  $C_F C_A$ , but terms proportional to  $C_F^2$  may be associated with a factorized contribution to the cross section, in which the gluon  $k$  is emitted coherently by the combinations of the gluon  $l$  and the eikonals. To generate the  $C_F C_A$  part, on the other hand, gluon  $k$  must “resolve” gluon  $l$  from the eikonal lines, giving a result that depends on the angles between  $\vec{l}$  and the eikonal directions.

The computation of the diagrams is outlined in Appendix A; here we quote the results. We adopt the notation  $c_l \equiv \cos \theta_l$ ,  $s_l \equiv \sin \theta_l$ , with  $\theta_l$  the angle of momentum  $\vec{l}$  measured relative to  $\vec{\beta}_1$ , and similarly for  $k$ . We take, as indicated above, a Laplace transform with respect to the shape variable, and identify the logarithm in the conjugate variable  $\nu$ . We find that the logarithmic  $C_F C_A$ -dependence of Fig. 3 may be written as a dimensionless eikonal cross section in terms of one energy and two polar angular integrals as

$$\begin{aligned} \frac{d\sigma_{\text{eik}}}{d\varepsilon} &= C_F C_A \left( \frac{\alpha_s}{\pi} \right)^2 \frac{1}{\varepsilon} \int_{-\sin \delta}^{\sin \delta} dc_k \int_{\sin \delta}^1 dc_l \int_{\varepsilon\sqrt{s}}^{\sqrt{s}} \frac{d\omega_l}{\omega_l} e^{-\nu \omega_l (1-c_l)^{1-a} s_l^a / Q} \\ &\times \left[ \frac{1}{c_k + c_l} \frac{1}{1 + c_k} \left( \frac{1}{1 + c_l} + \frac{1}{1 - c_k} \right) - \frac{1}{s_k^2} \frac{1}{1 + c_l} \right]. \end{aligned} \quad (15)$$

In this form, the absence of collinear singularities in the  $C_F C_A$  term at  $\cos \theta_l = +1$  is manifest, independent of  $\nu$ . Collinear singularities in the  $l$  integral completely factorize from the  $k$  integral,



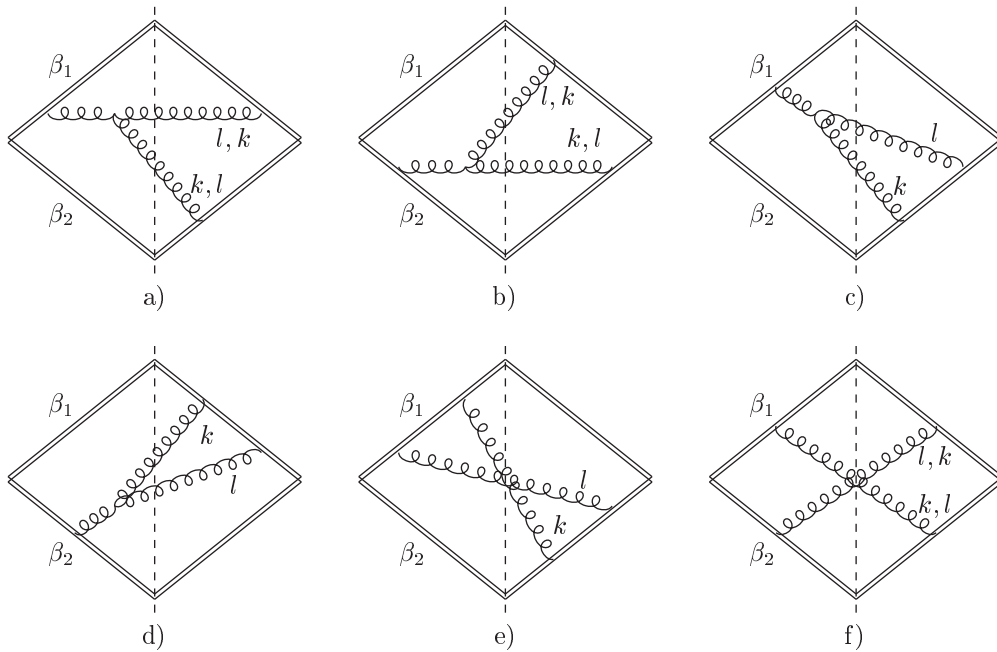


Figure 3: The relevant two-loop cut diagrams corresponding to the emission of two real gluons in the final state contributing to the eikonal cross section. The dashed line represents the final state, with contributions to the amplitude to the left, and to the complex conjugate amplitude to the right.

and are proportional to  $C_F^2$ . The logarithmic dependence on  $\varepsilon$  for  $\nu > 1$  is readily found to be

$$\frac{d\sigma_{\text{eik}}}{d\varepsilon} = C_F C_A \left(\frac{\alpha_s}{\pi}\right)^2 \frac{1}{\varepsilon} \ln\left(\frac{1}{\varepsilon\nu}\right) C(\Delta\eta), \quad (16)$$

where  $C(\Delta\eta)$  is a finite function of the angle  $\delta$ , given explicitly in Appendix A.

We can contrast this result to what happens when  $\nu = 0$ , that is, for an inclusive, non-global cross section. In this case, recalling that  $\varepsilon = Q_\Omega/Q$ , we find in place of Eq. (16) the non-global logarithm

$$\frac{d\sigma_{\text{eik}}}{d\varepsilon} = C_F C_A \left(\frac{\alpha_s}{\pi}\right)^2 \frac{1}{\varepsilon} \ln\left(\frac{Q}{Q_\Omega}\right) C(\Delta\eta). \quad (17)$$

As anticipated, the effect of the transform is to replace the non-global logarithm in  $Q/Q_\Omega$ , by a logarithm of  $1/(\varepsilon\nu)$ . We are now ready to generalize this result, starting from the factorization properties of the cross section near the two-jet limit.

### 3 Factorization of the Cross Section

In this section we study the factorization of the correlations (6). The analysis is based on a general approach that begins with the all-orders treatment of singularities in perturbative cross sections [24, 25], and derives factorization from the analyticity and gauge properties of high energy Green functions and cross sections [26]. The functions that appear in factorized cross sections are expressible in terms of QCD matrix elements [27], and the matrix elements that we will encounter are familiar from related analyses for heavy quark and jet production [28]. We refer in several places below to standard arguments discussed in more detail in [25, 26]. The aim of this section, and the reason why a careful analysis is necessary, is to identify the specific dimensionless combinations of kinematic variables on which the factorized matrix elements may depend. We will use these dependences in the following section, when we discuss the resummation properties of our correlations.

#### 3.1 Leading regions near the two-jet limit

In order to resum logarithms of  $\varepsilon$  and  $\bar{\varepsilon}$  (or equivalently  $\nu$ , the Laplace conjugate of  $\bar{\varepsilon}$ ) we have first to identify their origin in momentum space when  $\varepsilon, \bar{\varepsilon} \rightarrow 0$ . Following the procedure and terminology of [24], we identify “leading regions” in the momentum integrals of cut diagrams, which can give rise to logarithmic enhancements of the cross section associated with lines approaching the mass shell. Within these regions, the lines of a cut diagram fall into the following subdiagrams:

- A hard-scattering, or “short-distance” subdiagram  $H$ , where all components of line momenta are far off-shell, by order  $Q$ .

- Jet subdiagrams,  $J_1$  and  $J_2$ , where energies are fixed and momenta are collinear to the outgoing primary partons and the jet directions that emerge from the hard scattering. (For  $\varepsilon = \bar{\varepsilon} = 0$ , the sum of all energies in each jet is one-half the total energy.) To characterize the momenta of the lines within the jets, we introduce a scaling variable,  $\lambda \ll 1$ . Within jet 1, momenta  $\ell$  scale as ( $\ell^+ \sim Q, \ell^- \sim \lambda Q, \ell_\perp \sim \lambda^{1/2} Q$ ).
- A soft subdiagram,  $S$  connecting the jet functions  $J_1$  and  $J_2$ , in which the components of momenta  $k$  are small compared to  $Q$  in all components, scaling as ( $k^\pm \sim \lambda Q, k_\perp \sim \lambda Q$ ).

An arbitrary final state  $N$  is the union of substates associated with these subdiagrams:

$$N = N_s \oplus N_{J_1} \oplus N_{J_2}. \quad (18)$$

As a result, the event shape  $\bar{f}$  can also be written as a sum of contributions from the soft and jet subdiagrams:

$$\bar{f}(N, a) = \bar{f}^N(N_s, a) + \bar{f}_{\bar{\Omega}_1}^N(N_{J_1}, a) + \bar{f}_{\bar{\Omega}_2}^N(N_{J_2}, a). \quad (19)$$

The superscript  $N$  reminds us that the contributions of final-state particles associated with the soft and jet functions depend implicitly on the full final state, through the determination of the jet axes, as discussed in Sec. 2. In contrast, the energy flow weight,  $f(N)$ , depends only on particles emitted at wide angles, and is hence insensitive to collinear radiation:

$$f(N) = f(N_s). \quad (20)$$

When we sum over all diagrams that have a fixed final state, the contributions from these leading regions may be factorized into a set of functions, each of which corresponds to one of the generic hard, soft and jet subdiagrams. The arguments for this factorization at leading power have been discussed extensively [21, 26, 29]. The cross section becomes a convolution in  $\bar{\varepsilon}$ , with the sums over states linked by the delta function which fixes  $\hat{n}_1$ , and by momentum conservation,

$$\begin{aligned} \frac{d\bar{\sigma}(\varepsilon, \bar{\varepsilon}, s, a)}{d\varepsilon d\bar{\varepsilon} d\hat{n}_1} &= \frac{d\sigma_0}{d\hat{n}_1} H(s, \hat{n}_1) \sum_{N_s, N_{J_c}} \int d\bar{\varepsilon}_s \mathcal{S}(N_s) \delta(\varepsilon - f(N_s)) \delta(\bar{\varepsilon}_s - \bar{f}^N(N_s, a)) \\ &\quad \times \prod_{c=1}^2 \int d\bar{\varepsilon}_{J_c} \mathcal{J}_c(N_{J_c}) \delta(\bar{\varepsilon}_{J_c} - \bar{f}_{\bar{\Omega}_c}^N(N_{J_c}, a)) \\ &\quad \times (2\pi)^4 \delta^4(p_I - p(N_{J_2}) - p(N_{J_1}) - p(N_s)) \\ &\quad \times \delta^2(\hat{n}_1 - \hat{n}(N)) \delta(\bar{\varepsilon} - \bar{\varepsilon}_{J_1} - \bar{\varepsilon}_{J_2} - \bar{\varepsilon}_s) \\ &= \frac{d\sigma_0}{d\hat{n}_1} \delta(\varepsilon) \delta(\bar{\varepsilon}) + \mathcal{O}(\alpha_s). \end{aligned} \quad (21)$$

Here  $d\sigma_0/d\hat{n}_1$  is the Born cross section for the production of a single particle (quark or anti-quark) in direction  $\hat{n}_1$ , while the short-distance function  $H(s, \hat{n}_1) = 1 + \mathcal{O}(\alpha_s)$ , which describes corrections to the hard scattering, is an expansion in  $\alpha_s$  with finite coefficients. The functions

$\mathcal{J}_c(N_{J_c})$ ,  $\mathcal{S}(N_s)$  describe the internal dynamics of the jets and wide-angle soft radiation, respectively. We will specify these functions below. We have suppressed their dependence on a factorization scale. Radiation at wide angles from the jets will be well-described by our soft functions  $\mathcal{S}(N_s)$ , while we will construct the jet functions  $\mathcal{J}_c(N_{J_c})$  to be independent of  $\varepsilon$ , as in Eq. (21).

So far, we have specified our sums over states in Eq. (21) only when all lines in  $N_s$  are soft, and all lines in  $N_{J_c}$  have momenta that are collinear, or nearly collinear to  $p_{J_c}$ . As  $\varepsilon$  and  $\bar{\varepsilon}$  vanish, these are the only final-state momenta that are kinematically possible. Were we to restrict ourselves to these configurations only, however, it would not be straightforward to make the individual sums over  $N_s$  and  $N_{J_c}$  infrared safe. Thus, it is necessary to include soft partons in  $N_s$  that are emitted near the jet directions, and soft partons in the  $N_{J_c}$  at wide angles. We will show below how to define the functions  $\mathcal{J}_c(N_{J_c})$ ,  $\mathcal{S}(N_s)$  so that they generate factoring, infrared safe functions that avoid double counting. We know on the basis of the arguments of Refs. [21, 26, 29] that corrections to the factorization of soft from jet functions are suppressed by powers of the weight functions  $\varepsilon$  and/or  $\bar{\varepsilon}$ .

### 3.2 The factorization in convolution form

Although formally factorized, the jet and soft functions in Eq. (21) are still linked in a potentially complicated way through their dependence on the jet axes. Our strategy is to simplify this complex dependence to a simple convolution in contributions to  $\bar{\varepsilon}$ , accurate to leading power in  $\varepsilon$  and  $\bar{\varepsilon}$ .

First, we note that the cross section of Eq. (21) is singular for vanishing  $\varepsilon$  and  $\bar{\varepsilon}$ , but is a smooth function of  $s$  and  $\hat{n}_1$ . We may therefore make any approximation that changes  $s$  and/or  $\hat{n}_1$  by an amount that vanishes as a power of  $\varepsilon$  and  $\bar{\varepsilon}$  in the leading regions.

Correspondingly, the amplitudes for jet  $c$  are singular in  $\bar{\varepsilon}_{J_c}$ , but depend smoothly on the jet energy and direction, while the soft function is singular in both  $\varepsilon$  and  $\bar{\varepsilon}_s$ , but depends smoothly on the jet directions. As a result, at fixed values of  $\varepsilon$  and  $\bar{\varepsilon}$  we may approximate the jet directions and energies by their values at  $\varepsilon = \bar{\varepsilon} = 0$  in the soft and jet functions.

Finally, we may make any approximation that affects the value of  $\varepsilon$  and/or  $\bar{\varepsilon}_{J_c}$  by amounts that vanish faster than linearly for  $\bar{\varepsilon} \rightarrow 0$ . It is at this stage that we will require that  $a < 1$ .

With these observations in mind, we enumerate the replacements and approximations by which we reduce Eq. (21), while retaining leading-power accuracy.

1. To simplify the definitions of the jets in Eq. (21), we make the replacements  $\bar{f}_{\bar{\Omega}_c}^N(N_{J_c}, a) \rightarrow \bar{f}_c(N_{J_c}, a)$  with

$$\bar{f}_c(N_{J_c}, a) \equiv \frac{1}{\sqrt{s}} \sum_{\text{all } \hat{n}_i \in N_{J_c}} k_{i,\perp}^a \omega_i^{1-a} (1 - \hat{n}_i \cdot \hat{n}_c)^{1-a} . \quad (22)$$

The jet weight function  $\bar{f}_c(N_{J_c}, a)$  now depends only on particles associated with  $N_{J_c}$ . The contribution to  $\bar{f}_c(N_{J_c}, a)$  from particles within region  $\bar{\Omega}_c$ , is exactly the same here as in the weight (3), but we now include particles in all other directions. In this way, the independent

sums over final states of the jet amplitudes will be naturally infrared safe. The value of  $\bar{f}_c(N_{J_c}, a)$  differs from the value of  $\bar{f}_{\bar{\Omega}_c}^N(N_{J_c}, a)$ , however, due to radiation outside  $\bar{\Omega}_c$ , as indicated by the new subscript. This radiation is hence at wide angles to the jet axis. In the elastic limit (8), it is also constrained to be soft. Double counting in contributions to the total event shape,  $\bar{f}(N, a)$ , will be avoided by an appropriate definition of the soft function below. The sums over states are still not yet fully independent, however, because the jet directions  $\hat{n}_c$  still depend on the full final state  $N$ .

2. Next, we turn our attention to the condition that fixes the jet direction  $\hat{n}_1$ . Up to corrections in the orientation of  $\hat{n}_1$  that vanish as powers of  $\varepsilon$  and  $\bar{\varepsilon}$ , we may neglect the dependence of  $\hat{n}_1$  on  $N_s$  and  $N_{J_2}$ :

$$\delta(\hat{n}_1 - \hat{n}(N)) \rightarrow \delta(\hat{n}_1 - \hat{n}(N_{J_1})). \quad (23)$$

In Appendix B, we show that this replacement also leaves the value of  $\bar{\varepsilon}$  unchanged, up to corrections that vanish as  $\bar{\varepsilon}^{2-a}$ . Thus, for  $a < 1$ , (23) is acceptable to leading power. For  $a < 1$ , we can therefore identify the direction of jet 1 with  $\hat{n}_1$ . These approximations simplify Eq. (21) by eliminating the implicit dependence of the jet and soft weights on the full final state. We may now treat  $\hat{n}_1$  as an independent vector.

3. In the leading regions, particles that make up each final-state jet are associated with states  $N_{J_c}$ , while  $N_s$  consists of soft particles only. In the momentum conservation delta function, we can neglect the four-momenta of lines in  $N_s$ , whose energies all vanish as  $\varepsilon, \bar{\varepsilon} \rightarrow 0$ :

$$\delta^4(p_I - p(N_{J_2}) - p(N_{J_1}) - p(N_s)) \rightarrow \delta^4(p_I - p_{J_2} - p_{J_1}). \quad (24)$$

4. Because the cross section is a smooth function of the jet energies and directions, we may also neglect the masses of the jets within the momentum conservation delta function, as in Eq. (10). In this approximation, we derive in the c.m.,

$$\begin{aligned} \delta^4(p_I - p_{J_2} - p_{J_1}) &\rightarrow \delta(\sqrt{s} - \omega(N_{J_1}) - \omega(N_{J_2})) \delta(|\vec{p}_{J_1}| - |\vec{p}_{J_2}|) \frac{1}{|\vec{p}_{J_1}|^2} \delta^2(\hat{n}_1 + \hat{n}_2) \\ &\rightarrow \frac{2}{s} \delta\left(\frac{\sqrt{s}}{2} - \omega(N_{J_1})\right) \delta\left(\frac{\sqrt{s}}{2} - \omega(N_{J_2})\right) \delta^2(\hat{n}_1 + \hat{n}_2). \end{aligned} \quad (25)$$

Our jets are now back-to-back:

$$\hat{n}_2 \rightarrow -\hat{n}_1. \quad (26)$$

Implementing these replacements and approximations for  $a < 1$ , we rewrite the cross section Eq. (21) as

$$\begin{aligned} \frac{d\bar{\sigma}(\varepsilon, \bar{\varepsilon}, s, a)}{d\varepsilon d\bar{\varepsilon} d\hat{n}_1} &= \frac{d\sigma_0}{d\hat{n}_1} H(s, \hat{n}_1, \mu) \int d\bar{\varepsilon}_s \bar{S}(\varepsilon, \bar{\varepsilon}_s, a, \mu) \\ &\times \prod_{c=1}^2 \int d\bar{\varepsilon}_{J_c} \bar{J}_c(\bar{\varepsilon}_{J_c}, a, \mu) \delta(\bar{\varepsilon} - \bar{\varepsilon}_{J_1} - \bar{\varepsilon}_{J_2} - \bar{\varepsilon}_s), \end{aligned} \quad (27)$$

with (as above)  $H = 1 + \mathcal{O}(\alpha_s)$ . Referring to the notation of Eqs. (21) and (22), the functions  $\bar{S}$  and  $\bar{J}_c$  are:

$$\begin{aligned}\bar{S}(\varepsilon, \bar{\varepsilon}_s, a, \mu) &= \sum_{N_s} \mathcal{S}(N_s, \mu) \delta(\varepsilon - f(N_s)) \delta(\bar{\varepsilon}_s - \bar{f}(N_s, a)) \\ \bar{J}_c(\bar{\varepsilon}_{J_c}, a, \mu) &= \frac{2}{s} (2\pi)^6 \sum_{N_{J_c}} \mathcal{J}_c(N_{J_c}, \mu) \delta(\bar{\varepsilon}_{J_c} - \bar{f}_c(N_{J_c}, a)) \delta\left(\frac{\sqrt{s}}{2} - \omega(N_{J_c})\right) \delta^2(\hat{n}_1 \pm \hat{n}(N_{J_c})),\end{aligned}\tag{28}$$

$$\tag{29}$$

with the plus sign in the angular delta function for jet 2, and the minus for jet 1. The weight functions for the jets are given by Eq. (22) and induce dependence on the parameter  $a$ . We have introduced the factorization scale  $\mu$ , which we set equal to the renormalization scale.

We note that we must construct the soft functions  $\bar{S}(N_s, \mu)$  to cancel the contributions of final-state particles from each of the  $\bar{J}_c(N_{J_c}, \mu)$  to the weight  $\varepsilon$ , as well as the contributions of the jet functions to  $\bar{\varepsilon}$  from soft radiation outside their respective regions  $\bar{\Omega}_c$ . Similarly, the jet amplitudes must be constructed to include collinear enhancements only in their respective jet directions. Explicit constructions that satisfy these requirements will be specified in the following subsections.

To disentangle the convolution in (27), we take Laplace moments with respect to  $\bar{\varepsilon}$ :

$$\begin{aligned}\frac{d\sigma(\varepsilon, \nu, s, a)}{d\varepsilon d\hat{n}_1} &= \int_0^\infty d\bar{\varepsilon} e^{-\nu\bar{\varepsilon}} \frac{d\bar{\sigma}(\varepsilon, \bar{\varepsilon}, a)}{d\varepsilon d\bar{\varepsilon} d\hat{n}_1} \\ &= \frac{d\sigma_0}{d\hat{n}_1} H(s, \hat{n}_1, \mu) S(\varepsilon, \nu, a, \mu) \prod_{c=1}^2 J_c(\nu, a, \mu).\end{aligned}\tag{30}$$

Here and below unbarred quantities are the transforms in  $\bar{\varepsilon}$ , and barred quantities denote untransformed functions.

$$S(\varepsilon, \nu, a, \mu) = \int_0^\infty d\bar{\varepsilon}_s e^{-\nu\bar{\varepsilon}_s} \bar{S}(\varepsilon, \bar{\varepsilon}_s, a, \mu),\tag{31}$$

and similarly for the jet functions.

In the following subsections, we give explicit constructions for the functions participating in the factorization formula (27), which satisfy the requirement of infrared safety, and avoid double counting. An illustration of the cross section factorized into these functions is shown in Fig. 4. As discussed above, non-global logarithms will emerge when  $\varepsilon\nu$  becomes small enough.

### 3.3 The short-distance function

The power counting described in [24] shows that in Feynman gauge the subdiagrams of Fig. 4 that contribute to  $H$  in Eq. (27) at leading power in  $\varepsilon$  and  $\bar{\varepsilon}$  are connected to each of the two jet subdiagrams by a single on-shell quark line, along with a possible set of on-shell, collinear gluon lines that carry scalar polarizations. The hard subdiagram is not connected directly to the soft subdiagram in any leading region.

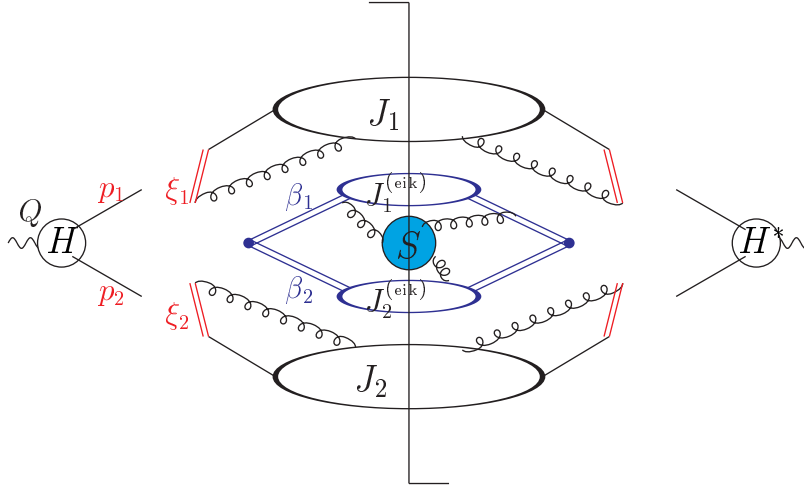


Figure 4: Factorized cross section (27) after the application of Ward identities. The vertical line denotes the final state cut.

The couplings of the scalar-polarized gluons that connect the jets with short-distance sub-diagrams may be simplified with the help of Ward identities (see, e. g. [26]). At each order of perturbation theory, the coupling of scalar-polarized gluons from either jet to the short-distance function is equivalent to their coupling to a path-ordered exponential of the gauge field, oriented in any direction that is not collinear to the jet. Corrections are infrared safe, and can be absorbed into the short-distance function. Let  $h(p_{J_c}, \hat{n}_1, \mathcal{A})$  represent the set of all short-distance contributions to diagrams that couple any number of scalar-polarized gluons to the jets, in the amplitude for the production of any final state. The argument  $\mathcal{A}$  stands for the fields that create the scalar-polarized gluons linking the short-distance function to the jets. On a diagram-by-diagram basis,  $h$  depends on the momentum of each of the scalar-polarized gluons. After the sum over all diagrams, however, we can make the replacement:

$$h(p_{J_c}, \hat{n}_1, \mathcal{A}^{(q, \bar{q})}) \rightarrow \Phi_{\xi_2}^{(\bar{q})}(0, -\infty; 0) h_2(p_{J_c}, \hat{n}_1, \xi_c) \Phi_{\xi_1}^{(q)}(0, -\infty; 0), \quad (32)$$

where  $h_2$  is a short-distance function that depends only on the total momenta  $p_{J_1}$  and  $p_{J_2}$ . It also depends on vectors  $\xi_c$  that characterize the path-ordered exponentials  $\Phi(0, -\infty; 0)$ :

$$\Phi_{\xi_c}^{(f)}(0, -\infty; 0) = P e^{-ig \int_{-\infty}^0 d\lambda \xi_c \cdot \mathcal{A}^{(f)}(\lambda \xi_c)}, \quad (33)$$

where the superscript (f) indicates that the vector potential takes values in representation f, in our case the representation of a quark or antiquark. These operators will be associated with gauge-invariant definitions of the jet functions below. To avoid spurious collinear singularities, we choose the vectors  $\xi_c$ ,  $c = 1, 2$ , off the light cone. In the full cross section (30) the  $\xi_c$ -dependence cancels, of course.

The dimensionless short-distance function  $H = |h_2|^2$  in Eq. (27) depends on  $\sqrt{s}$  and  $p_{J_c} \cdot \xi_c$ , but not on any variable that vanishes with  $\varepsilon$  and  $\bar{\varepsilon}$ :

$$H(p_{J_c}, \xi_c, \hat{n}_1, \mu) = H\left(\frac{\sqrt{s}}{\mu}, \frac{p_{J_c} \cdot \hat{\xi}_c}{\mu}, \hat{n}_1, \alpha_s(\mu)\right), \quad (34)$$

where

$$\hat{\xi}_c \equiv \xi_c / \sqrt{|\xi_c^2|}. \quad (35)$$

Here we have observed that each diagram is independent of the overall scale of the eikonal vector  $\xi_c^\mu$ .

### 3.4 The jet functions

The jet functions and the soft functions in Eq. (27) can be defined in terms of specific matrix elements, which absorb the relevant contributions to leading regions in the cross section, and which are infrared safe. Their perturbative expansions specify the functions  $\mathcal{S}$  and  $\mathcal{J}_c$  of Eq. (29). We begin with our definition of the jet functions.

The jet functions, which absorb enhancements collinear to the two outgoing particles produced in the primary hard scattering, can be defined in terms of matrix elements in a manner reminiscent of parton distribution or decay functions [27]. To be specific, we consider the quark jet function:

$$\begin{aligned} \bar{J}_c^{\mu}( \bar{\varepsilon}_{J_c}, a, \mu ) &= \frac{2}{s} \frac{(2\pi)^6}{\mathcal{N}_C} \sum_{N_{J_c}} \text{Tr} \left[ \gamma^\mu \langle 0 | \Phi_{\xi_c}^{(q)\dagger}(0, -\infty; 0) q(0) | N_{J_c} \rangle \langle N_{J_c} | \bar{q}(0) \Phi_{\xi_c}^{(q)}(0, -\infty; 0) | 0 \rangle \right] \\ &\quad \times \delta(\bar{\varepsilon}_{J_c} - \bar{f}_c(N_{J_c}, a)) \delta\left(\frac{\sqrt{s}}{2} - \omega(N_{J_c})\right) \delta^2(\hat{n}_c - \hat{n}(N_{J_c})), \end{aligned} \quad (36)$$

where  $\mathcal{N}_C$  is the number of colors, and where  $\hat{n}_c$  denotes the direction of the momentum of jet  $c$ , Eq. (29), with  $\hat{n}_2 = -\hat{n}_1$ .  $q$  is the quark field,  $\Phi_{\xi_c}^{(q)}(0, -\infty; 0)$  a path-ordered exponential in the notation of (33), and the trace is taken over color and Dirac indices. We have chosen the normalization so that the jet functions  $\bar{J}^{\mu}$  in (36) are dimensionless and begin at lowest order with

$$\bar{J}_c^{\mu(0)}(\bar{\varepsilon}_{J_c}, a, \mu) = \beta_c^\mu \delta(\bar{\varepsilon}_{J_c}), \quad (37)$$

with  $\beta_c^\mu$  the lightlike velocities corresponding to the jet momenta in Eq. (10):

$$\beta_1^\mu = \delta_{\mu+}, \quad \beta_2^\mu = \delta_{\mu-}. \quad (38)$$

The scalar jet functions of Eq. (29) are now obtained by projecting out the component of  $J_c^\mu$  in the jet direction:

$$\bar{J}_c(\bar{\varepsilon}_{J_c}, a, \mu) = \bar{\beta}_c \cdot \bar{J}'_c(\bar{\varepsilon}_{J_c}, a, \mu) = \delta(\bar{\varepsilon}_{J_c}) + \mathcal{O}(\alpha_s), \quad (39)$$

where  $\bar{\beta}_1 = \beta_2$ ,  $\bar{\beta}_2 = \beta_1$  are the lightlike vectors in the directions opposite to  $\beta_1$  and  $\beta_2$ , respectively. By construction, the  $\bar{J}_c$  are linear in  $\bar{\beta}_c$ .



To resum the jet functions in the variables  $\bar{\varepsilon}_{J_c}$ , it is convenient to reexpress the weight functions (22) in combinations of light-cone momentum components that are invariant under boosts in the  $x_3$  direction,

$$\begin{aligned}\bar{f}_1(N_{J_1}, a) &= \frac{1}{s^{1-a/2}} \sum_{\hat{n}_i \in N_{J_1}} k_{i,\perp}^a \left(2p_{J_1}^+ k_i^-\right)^{1-a}, \\ \bar{f}_2(N_{J_2}, a) &= \frac{1}{s^{1-a/2}} \sum_{\hat{n}_i \in N_{J_2}} k_{i,\perp}^a \left(2p_{J_2}^- k_i^+\right)^{1-a}.\end{aligned}\quad (40)$$

Here we have used the relation  $\sqrt{s}/2 = \omega_{J_c}$ , valid for both jets in the c.m. At the same time, we make the identification,

$$\frac{1}{s} \delta\left(\frac{\sqrt{s}}{2} - \omega(N_{J_c})\right) \delta^2(\hat{n}_c - \hat{n}(N_{J_c})) = \frac{1}{4} \delta^3(\vec{p}_{J_c} - \vec{p}(N_{J_c})), \quad (41)$$

which again holds in the c.m. frame. The spatial components of each  $p_{J_c}$  are thus fixed. Given that we are at small  $\bar{\varepsilon}_{J_c}$ , the jet functions may be thought of as functions of the light-like jet momenta  $p_{J_c}^\mu$  of Eq. (10) and of  $\bar{\varepsilon}_{J_c}$ . Because the vector jet function is constructed to be dimensionless,  $\bar{J}'_c$  in Eq. (36) is proportional to  $\beta_c$  rather than  $p_{J_c}$ . Otherwise, it is free of explicit  $\beta_c$ -dependence.

The jet functions can now be written in terms of boost-invariant arguments, homogeneous of degree zero in  $\xi_c$ :

$$\begin{aligned}\bar{J}_c(\bar{\varepsilon}_{J_c}, a, \mu) &= \bar{\beta}_{c\mu} \left[ \beta_c^\mu \bar{J}_c^{(1)}\left(\frac{p_{J_c} \cdot \hat{\xi}_c}{\mu}, \bar{\varepsilon}_{J_c} \frac{\sqrt{s}}{\mu} \left(\frac{\sqrt{s}}{2p_{J_c} \cdot \hat{\xi}_c}\right)^{1-a}, a, \alpha_s(\mu)\right) \right. \\ &\quad \left. + \frac{2\xi_c^\mu \beta_c \cdot \xi_c}{|\xi_c|^2} \bar{J}_c^{(2)}\left(\frac{p_{J_c} \cdot \hat{\xi}_c}{\mu}, \bar{\varepsilon}_{J_c} \frac{\sqrt{s}}{\mu} \left(\frac{\sqrt{s}}{2p_{J_c} \cdot \hat{\xi}_c}\right)^{1-a}, a, \alpha_s(\mu)\right) \right],\end{aligned}\quad (42)$$

where  $\bar{J}^{(1)}$  and  $\bar{J}^{(2)}$  are independent functions, and where we have suppressed possible dependence on  $\hat{\xi}_{c,\perp}$ . For jet  $c$ , the weight  $\bar{\varepsilon}_{J_c}$  is fixed by  $\delta(\bar{\varepsilon}_{J_c} - \bar{f}_c(N_{J_c}, a))$ , where on the right-hand side of the expression for the weight (40), the sum over each particle's momentum involves the overall factor  $(2p_{J_c}^\pm/\sqrt{s})^{1-a}$ . After integration over final states at fixed  $\bar{\varepsilon}_{J_c}$ , the jet can thus depend on the vector  $p_{J_c}^\mu$ . At the same time, it is easy to see from the definition of the weight that  $p_{J_c}^\mu$  can only appear in the combination  $(1/\bar{\varepsilon}_{J_c}\sqrt{s})^{1/(1-a)} (2p_{J_c}^\mu/\sqrt{s})$ . This vector can combine with  $\xi_c$  to form an invariant, and all  $\xi_c$ -dependence comes about in this way.

Expression (42) can be further simplified by noting that

$$2\bar{\beta}_c \cdot \xi_c \beta_c \cdot \xi_c = \xi_c^2 + \xi_{c,\perp}^2. \quad (43)$$

Choosing  $\xi_{c,\perp} = 0$ , we find a single combination,

$$\bar{J}_c(\bar{\varepsilon}_{J_c}, a, \mu) = \bar{J}_c\left(\frac{p_{J_c} \cdot \hat{\xi}_c}{\mu}, \bar{\varepsilon}_{J_c} \frac{\sqrt{s}}{\mu} (\xi_c)^{1-a}, a, \alpha_s(\mu)\right), \quad (44)$$

where, in the notation of Eq. (42),  $\bar{J}_c = \bar{J}_c^{(1)} + \bar{J}_c^{(2)}$ , and we have defined

$$\zeta_c \equiv \frac{\sqrt{s}}{2p_{J_c} \cdot \hat{\xi}_c}. \quad (45)$$

In these terms, the Laplace moments of the jet function inherit dependence on the moment variable  $\nu$  through

$$\begin{aligned} J_c(\nu, a, \mu) &= \int_0^\infty d\bar{\varepsilon}_{J_c} e^{-\nu \bar{\varepsilon}_{J_c}} \bar{J}_c(\bar{\varepsilon}_{J_c}, a, \mu) \\ &\equiv J_c\left(\frac{p_{J_c} \cdot \hat{\xi}_c}{\mu}, \frac{\sqrt{s}}{\mu\nu} (\zeta_c)^{1-a}, a, \alpha_s(\mu)\right), \end{aligned} \quad (46)$$

where the unbarred and barred quantities denote transformed and untransformed functions, respectively. We have constructed the jet functions to be independent of  $\varepsilon$ , since the radiation into  $\Omega$  is at wide angles from the jet axes and can therefore be completely factored from the collinear radiation. This radiation at wide angles is contained in the soft function, which will be defined below in a manner that avoids double counting in the cross section.

### 3.5 The soft function

Given the definitions for the jet functions in the previous subsection, and the factorization (27), we may in principle calculate the soft function  $S$  order by order in perturbation theory. We can derive a more explicit definition of the soft function, however, by relating it to an eikonal analog of Eq. (27).

As reviewed in Refs. [15, 26], soft radiation at wide angles from the jets decouples from the collinear lines within the jet. As a result, to compute amplitudes for wide-angle radiation, the jets may be replaced by nonabelian phases, or Wilson lines. We therefore construct a dimensionless quantity,  $\sigma^{(\text{eik})}$ , in which gluons are radiated by path-ordered exponentials  $\Phi$ , which mimic the color flow of outgoing quarks,

$$\Phi_{\beta_c}^{(f)}(\infty, 0; x) = P e^{-ig \int_0^\infty d\lambda \beta_c \cdot \mathcal{A}^{(f)}(\lambda \beta_c + x)}, \quad (47)$$

with  $\beta_c$  a light-like velocity in either of the jet directions. For the two-jet cross section at measured  $\varepsilon$  and  $\bar{\varepsilon}_{\text{eik}}$ , we define

$$\begin{aligned} \bar{\sigma}^{(\text{eik})}(\varepsilon, \bar{\varepsilon}_{\text{eik}}, a, \mu) &\equiv \frac{1}{\mathcal{N}_C} \sum_{N_{\text{eik}}} \langle 0 | \Phi_{\beta_2}^{(\bar{q})\dagger}(\infty, 0; 0) \Phi_{\beta_1}^{(q)\dagger}(\infty, 0; 0) | N_{\text{eik}} \rangle \\ &\quad \times \langle N_{\text{eik}} | \Phi_{\beta_1}^{(q)}(\infty, 0; 0) \Phi_{\beta_2}^{(\bar{q})}(\infty, 0; 0) | 0 \rangle \delta(\varepsilon - f(N_{\text{eik}})) \delta(\bar{\varepsilon}_{\text{eik}} - \bar{f}(N_{\text{eik}}, a)) \\ &= \delta(\varepsilon) \delta(\bar{\varepsilon}_{\text{eik}}) + \mathcal{O}(\alpha_s). \end{aligned} \quad (48)$$

The sum is over all final states  $N_{\text{eik}}$  in the eikonal cross section. The renormalization scale in this cross section, which will also serve as a factorization scale, is denoted  $\mu$ . Here the event

shape function  $\bar{\varepsilon}_{\text{eik}}$  is defined by  $\bar{f}(N_{\text{eik}}, a)$  as in Eqs. (3) and (4), distinguishing between the hemispheres around the jets. As usual,  $\mathcal{N}_C$  is the number of colors, and a trace over color is understood.

The eikonal cross section (48) models the soft radiation away from the jets, including the radiation into  $\Omega$ , accurately. It also contains enhancements for configurations collinear to the jets, which, however, are already taken into account by the partonic jet functions in (27). Indeed, (48) does not reproduce the partonic cross section accurately for collinear radiation. It is also easy to verify at lowest order that even at fixed  $\bar{\varepsilon}_{\text{eik}}$  the eikonal cross section (48) is ultraviolet divergent in dimensional regularization, unless we also impose a cutoff on the energy of real gluon emission collinear to  $\beta_1$  or  $\beta_2$ .

The construction of the soft function  $S$  from  $\bar{\sigma}^{(\text{eik})}$  is nevertheless possible because the eikonal cross section (48) factorizes in the same manner as the cross section itself, into eikonal jet functions and a soft function. The essential point [14] is that the soft function in the factorized eikonal cross section is the same as in the original cross section (27). The eikonal jets organize all collinear enhancements in (48), including the spurious ultraviolet divergences. These eikonal jet functions are defined analogously to their partonic counterparts, Eq. (36), but now with ordered exponentials replacing the quark fields,

$$\begin{aligned} \bar{J}_c^{(\text{eik})}(\bar{\varepsilon}_c, a, \mu) &\equiv \frac{1}{\mathcal{N}_C} \sum_{N_c^{(\text{eik})}} \langle 0 | \Phi_{\xi_c}^{(f_c)\dagger}(0, -\infty; 0) \Phi_{\beta_c}^{(f_c)\dagger}(\infty, 0; 0) | N_c^{(\text{eik})} \rangle \\ &\quad \langle N_c^{(\text{eik})} | \Phi_{\beta_c}^{(f_c)}(\infty, 0; 0) \Phi_{\xi_c}^{(f_c)}(0, -\infty; 0) | 0 \rangle \delta(\bar{\varepsilon}_c - \bar{f}_c(N_c^{(\text{eik})}, a)) \\ &= \delta(\bar{\varepsilon}_c) + \mathcal{O}(\alpha_s), \end{aligned} \quad (49)$$

where  $f_c$  is a quark or antiquark, and where the trace over color is understood. The weight functions are given as above, by Eq. (22), with the sum over particles in all directions.

In terms of the eikonal jets, the eikonal cross section (48) factorizes as

$$\bar{\sigma}^{(\text{eik})}(\varepsilon, \bar{\varepsilon}_{\text{eik}}, a, \mu) \equiv \int d\bar{\varepsilon}_s \bar{S}(\varepsilon, \bar{\varepsilon}_s, a, \mu) \prod_{c=1}^2 \int d\bar{\varepsilon}_c \bar{J}_c^{(\text{eik})}(\bar{\varepsilon}_c, a, \mu) \delta(\bar{\varepsilon}_{\text{eik}} - \bar{\varepsilon}_s - \bar{\varepsilon}_1 - \bar{\varepsilon}_2), \quad (50)$$

where we pick the factorization scale equal to the renormalization scale  $\mu$ . As for the full cross section, the convolution in (50) is simplified by a Laplace transformation (46) with respect to  $\bar{\varepsilon}_{\text{eik}}$ , which allows us to solve for the soft function as

$$S(\varepsilon, \nu, a, \mu) = \frac{\sigma^{(\text{eik})}(\varepsilon, \nu, a, \mu)}{\prod_{c=1}^2 J_c^{(\text{eik})}(\nu, a, \mu)} = \delta(\varepsilon) + \mathcal{O}(\alpha_s). \quad (51)$$

In this ratio, collinear logarithms in  $\nu$  and the unphysical ultraviolet divergences and their associated cutoff dependence cancel between the eikonal cross section and the eikonal jets, leaving a soft function that is entirely free of collinear enhancements. The soft function retains  $\nu$ -dependence through soft emission, which is also restricted by the weight function  $\varepsilon$ . In addition, because soft radiation within the eikonal jets can be factored from its collinear radiation, just as in the

partonic jets, all logarithms in  $\nu$  associated with wide-angle radiation are identical between the partonic and eikonal jets, and factor from logarithmic corrections associated with collinear radiation in both cases. As a result, the inverse eikonal jet functions cancel contributions from the wide-angle soft radiation of the partonic jets in the transformed cross section (30).

Given the definition of the energy flow weight function  $f$ , Eq. (5), the soft function is not boost invariant. In addition, because it is free of collinear logs, it can have at most a single logarithm per loop. Its dependence on  $\varepsilon$  is therefore only through ratios of the dimensional quantities  $\varepsilon\sqrt{s}$  with the renormalization (factorization) scale.

As in the case of the partonic jets, Eq. (46), we need to identify the variable through which  $\nu$  appears in the soft function. We note that dependence on the velocity vectors  $\beta_c$  and the factorization vectors  $\xi_c$  must be scale invariant in each, since they arise only from eikonal lines and vertices. The eikonal jet functions cannot depend explicitly on the scale-less, lightlike eikonal velocities  $\beta_c$ , and  $\sigma^{(\text{eik})}$  is independent of the  $\xi_c$ . Dependence on the factorization vectors  $\xi_c$  enters only through the weight functions, (40) for the eikonal jets, in a manner analogous to the case of the partonic jets. This results in a dependence on  $(\zeta_c)^{1-a}$ , as above, with  $\zeta_c$  defined in Eq. (45). In summary, we may characterize the arguments of the soft function in transform space as

$$S(\varepsilon, \nu, a, \mu) = S\left(\frac{\varepsilon\sqrt{s}}{\mu}, \varepsilon\nu, \frac{\sqrt{s}}{\mu\nu} (\zeta_c)^{1-a}, a, \alpha_s(\mu)\right). \quad (52)$$

## 4 Resummation

We may summarize the results of the previous section by rewriting the transform of the factorized cross section (30) in terms of the hard, jet and soft functions identified above, which depend on the kinematic variables and the moment  $\nu$  according to Eqs. (34), (46) and (52) respectively,

$$\begin{aligned} \frac{d\sigma(\varepsilon, \nu, s, a)}{d\varepsilon d\hat{n}_1} &= \frac{d\sigma_0}{d\hat{n}_1} H\left(\frac{\sqrt{s}}{\mu}, \frac{p_{J_c} \cdot \hat{\xi}_c}{\mu}, \hat{n}_1, \alpha_s(\mu)\right) \prod_{c=1}^2 J_c\left(\frac{p_{J_c} \cdot \hat{\xi}_c}{\mu}, \frac{\sqrt{s}}{\mu\nu} (\zeta_c)^{1-a}, a, \alpha_s(\mu)\right) \\ &\times S\left(\frac{\varepsilon\sqrt{s}}{\mu}, \varepsilon\nu, \frac{\sqrt{s}}{\mu\nu} (\zeta_c)^{1-a}, a, \alpha_s(\mu)\right). \end{aligned} \quad (53)$$

The natural scale for the strong coupling in the short-distance function  $H$  is  $\sqrt{s}/2$ . Setting  $\mu = \sqrt{s}/2$ , however, introduces large logarithms of  $\varepsilon$  in the soft function and large logarithms of  $\nu$  in both the soft and jet functions. The purpose of this section is to control these logarithms by the identification and solution of renormalization group and evolution equations.

The information necessary to perform the resummations is already present in the factorization (53). The cross section itself is independent of the factorization scale

$$\mu \frac{d}{d\mu} \frac{d\sigma(\varepsilon, \nu, s, a)}{d\varepsilon d\hat{n}_1} = 0, \quad (54)$$

and of the choice of the eikonal directions,  $\hat{\xi}_c$ , used in the factorization,

$$\frac{\partial}{\partial \ln(p_{J_c} \cdot \hat{\xi}_c)} \frac{d\sigma(\varepsilon, \nu, s, a)}{d\varepsilon d\hat{n}_1} = 0. \quad (55)$$

The arguments of this section closely follow the analysis of Ref. [30]. We will see that the dependence of jet and soft functions on the parameter  $a$  that characterizes the event shapes (3) is reflected in the resummed correlations, so that the relationship between correlations with different values of  $a$  is both calculable and nontrivial.

## 4.1 Energy flow

As a first step, we use the renormalization group equation (54) to organize dependence on the energy flow variable  $\varepsilon$ . Applying Eq. (54) to the factorized correlation (53), we derive the following consistency conditions, which are themselves renormalization group equations:

$$\mu \frac{d}{d\mu} \ln S \left( \frac{\varepsilon \sqrt{s}}{\mu}, \varepsilon \nu, \frac{\sqrt{s}}{\mu \nu} (\zeta_c)^{1-a}, a, \alpha_s(\mu) \right) = -\gamma_s(\alpha_s(\mu)), \quad (56)$$

$$\mu \frac{d}{d\mu} \ln J_c \left( \frac{p_{J_c} \cdot \hat{\xi}_c}{\mu}, \frac{\sqrt{s}}{\mu \nu} (\zeta_c)^{1-a}, a, \alpha_s(\mu) \right) = -\gamma_{J_c}(\alpha_s(\mu)), \quad (57)$$

$$\mu \frac{d}{d\mu} \ln H \left( \frac{\sqrt{s}}{\mu}, \frac{p_{J_c} \cdot \hat{\xi}_c}{\mu}, \hat{n}_1, \alpha_s(\mu) \right) = \gamma_s(\alpha_s(\mu)) + \sum_{c=1}^2 \gamma_{J_c}(\alpha_s(\mu)). \quad (58)$$

The anomalous dimensions  $\gamma_d$ ,  $d = s, J_c$  can depend only on variables held in common between at least two of the functions. Because each function is infrared safe, while ultraviolet divergences are present only in virtual diagrams, the anomalous dimensions cannot depend on the parameters  $\nu$ ,  $\varepsilon$  or  $a$ . This leaves as arguments of the  $\gamma_d$  only the coupling  $\alpha_s(\mu)$ , which we exhibit, and  $\zeta_c$ , which we suppress for now.

Solving Eqs. (56) and (57) we find

$$S \left( \frac{\varepsilon \sqrt{s}}{\mu}, \varepsilon \nu, \frac{\sqrt{s}}{\mu \nu} (\zeta_c)^{1-a}, a, \alpha_s(\mu) \right) = S \left( \frac{\varepsilon \sqrt{s}}{\mu_0}, \varepsilon \nu, \frac{\sqrt{s}}{\mu_0 \nu} (\zeta_c)^{1-a}, a, \alpha_s(\mu_0) \right) e^{-\int_{\mu_0}^{\mu} \frac{d\lambda}{\lambda} \gamma_s(\alpha_s(\lambda))}, \quad (59)$$

$$J_c \left( \frac{p_{J_c} \cdot \hat{\xi}_c}{\mu}, \frac{\sqrt{s}}{\mu \nu} (\zeta_c)^{1-a}, a, \alpha_s(\mu) \right) = J_c \left( \frac{p_{J_c} \cdot \hat{\xi}_c}{\tilde{\mu}_0}, \frac{\sqrt{s}}{\tilde{\mu}_0 \nu} (\zeta_c)^{1-a}, a, \alpha_s(\tilde{\mu}_0) \right) e^{-\int_{\tilde{\mu}_0}^{\mu} \frac{d\lambda}{\lambda} \gamma_{J_c}(\alpha_s(\lambda))}, \quad (60)$$

for the soft and jet functions. As suggested above, we will eventually pick  $\mu \sim \sqrt{s}$  to avoid large logs in  $H$ . Using these expressions in Eq. (53) we can avoid logarithms of  $\varepsilon$  or  $\nu$  in the soft function, by evolving from  $\mu_0 = \varepsilon \sqrt{s}$  to the factorization scale  $\mu \sim \sqrt{s}$ . No choice of  $\tilde{\mu}_0$ , however, controls all logarithms of  $\nu$  in the jet functions. Leaving  $\tilde{\mu}_0$  free, we find for the cross section (53) the intermediate result

$$\frac{d\sigma(\varepsilon, \nu, s, a)}{d\varepsilon d\hat{n}_1} = \frac{d\sigma_0}{d\hat{n}_1} H \left( \frac{\sqrt{s}}{\mu}, \frac{p_{J_c} \cdot \hat{\xi}_c}{\mu}, \hat{n}_1, \alpha_s(\mu) \right)$$

$$\begin{aligned}
& \times S \left( 1, \varepsilon\nu, (\zeta_c)^{1-a}, a, \alpha_s(\varepsilon\sqrt{s}) \right) \exp \left\{ - \int_{\varepsilon\sqrt{s}}^{\mu} \frac{d\lambda}{\lambda} \gamma_s(\alpha_s(\lambda)) \right\} \\
& \times J_c \left( \frac{p_{J_c} \cdot \hat{\xi}_c}{\tilde{\mu}_0}, \frac{\sqrt{s}}{\tilde{\mu}_0\nu} (\zeta_c)^{1-a}, a, \alpha_s(\tilde{\mu}_0) \right) \exp \left\{ - \int_{\tilde{\mu}_0}^{\mu} \frac{d\lambda}{\lambda} \gamma_{J_c}(\alpha_s(\lambda)) \right\}.
\end{aligned} \tag{61}$$

We have avoided introducing logarithms of  $\varepsilon$  into the jet functions, which originally only depend on  $\nu$ , by evolving the soft and the jet functions independently. The choice of  $\mu_0 = \varepsilon\sqrt{s}$  or  $\sqrt{s}/\nu$  for the soft function is to some extent a matter of convenience, since the two choices differ by logarithms of  $\varepsilon\nu$ . In general, if we choose  $\mu_0 = \sqrt{s}/\nu$ , logarithms of  $\varepsilon\nu$  will appear multiplied by coefficients that reflect the size of region  $\Omega$ . An example is Eq. (15) above. When  $\Omega$  has a small angular size,  $\mu_0 = \sqrt{s}/\nu$  is generally the more natural choice, since then logarithms in  $\varepsilon\nu$  will enter with small weights. In contrast, when  $\Omega$  grows to cover most angular directions, as in the study of rapidity gaps [32], it is more natural to choose  $\mu_0 = \varepsilon\sqrt{s}$ .

## 4.2 Event shape transform

The remaining unorganized “large” logarithms in (61), are in the jet functions, which we will resum by using the consistency equation (55). The requirement that the cross section be independent of  $p_{J_c} \cdot \hat{\xi}_c$  implies that the jet, soft and hard functions obey equations analogous to (56)–(58), again in terms of the variables that they hold in common [30]. The same results may be derived following the method of Collins and Soper [21], by defining the jets in an axial gauge, and then studying their variations under boosts.

For our purposes, only the equation satisfied by the jet functions [21, 30] is necessary,

$$\begin{aligned}
& \frac{\partial}{\partial \ln(p_{J_c} \cdot \hat{\xi}_c)} \ln J_c \left( \frac{p_{J_c} \cdot \hat{\xi}_c}{\mu}, \frac{\sqrt{s}}{\mu\nu} (\zeta_c)^{1-a}, a, \alpha_s(\mu) \right) \\
& = K_c \left( \frac{\sqrt{s}}{\mu\nu} (\zeta_c)^{1-a}, a, \alpha_s(\mu) \right) + G_c \left( \frac{p_{J_c} \cdot \hat{\xi}_c}{\mu}, \alpha_s(\mu) \right).
\end{aligned} \tag{62}$$

The functions  $K_c$  and  $G_c$  compensate the  $\xi_c$ -dependence of the soft and hard functions, respectively, which determines the kinematic variables upon which they may depend. In particular, notice the combination of  $\nu$ - and  $\xi_c$ -dependence required by the arguments of the jet function, Eq. (46).

Since the definition of our jet functions (36) is gauge invariant, we can derive the kernels  $K_c$  and  $G_c$  by an explicit computation of  $\partial J_c / \partial \ln(p_{J_c} \cdot \hat{\xi}_c)$  in any gauge. The multiplicative renormalizability of the jet function, Eq. (57), with an anomalous dimension that is independent of  $p_{J_c} \cdot \hat{\xi}_c$  ensures that the right-hand side of Eq. (62) is a renormalization-group invariant. Thus,  $K_c + G_c$  are renormalized additively, and satisfy [21]

$$\mu \frac{d}{d\mu} K_c \left( \frac{\sqrt{s}}{\mu\nu} (\zeta_c)^{1-a}, a, \alpha_s(\mu) \right) = -\gamma_{K_c}(\alpha_s(\mu)),$$

$$\mu \frac{d}{d\mu} G_c \left( \frac{p_{J_c} \cdot \hat{\xi}_c}{\mu}, \alpha_s(\mu) \right) = \gamma_{K_c}(\alpha_s(\mu)). \quad (63)$$

Since  $G_c$  and hence  $\gamma_{K_c}$ , may be computed from virtual diagrams, they do not depend on  $a$ , and  $\gamma_{K_c}$  is the universal Sudakov anomalous dimension [21, 33].

With the help of these evolution equations, the terms  $K_c$  and  $G_c$  in Eq. (62) can be reexpressed as [34]

$$\begin{aligned} & K_c \left( \frac{\sqrt{s}}{\mu \nu} (\zeta_c)^{1-a}, a, \alpha_s(\mu) \right) + G_c \left( \frac{p_{J_c} \cdot \hat{\xi}_c}{\mu}, \alpha_s(\mu) \right) \\ &= K_c \left( \frac{1}{c_1}, a, \alpha_s \left( c_1 \frac{\sqrt{s}}{\nu} (\zeta_c)^{1-a} \right) \right) + G_c \left( \frac{1}{c_2}, \alpha_s \left( c_2 p_{J_c} \cdot \hat{\xi}_c \right) \right) - \int_{c_1 \sqrt{s} (\zeta_c)^{1-a}/\nu}^{c_2 p_{J_c} \cdot \hat{\xi}_c} \frac{d\lambda'}{\lambda'} \gamma_{K_c}(\alpha_s(\lambda')) \\ &= -B'_c \left( c_1, c_2, a, \alpha_s \left( c_2 p_{J_c} \cdot \hat{\xi}_c \right) \right) - 2 \int_{c_1 \sqrt{s} (\zeta_c)^{1-a}/\nu}^{c_2 p_{J_c} \cdot \hat{\xi}_c} \frac{d\lambda'}{\lambda'} A'_c \left( c_1, a, \alpha_s(\lambda') \right), \end{aligned} \quad (64)$$

where in the second equality we have shifted the argument of the running coupling in  $K_c$ , and have introduced the notation

$$\begin{aligned} B'_c(c_1, c_2, a, \alpha_s(\mu)) &\equiv -K_c \left( \frac{1}{c_1}, a, \alpha_s(\mu) \right) - G_c \left( \frac{1}{c_2}, \alpha_s(\mu) \right), \\ 2A'_c(c_1, a, \alpha_s(\mu)) &\equiv \gamma_{K_c}(\alpha_s(\mu)) + \beta(g(\mu)) \frac{\partial}{\partial g(\mu)} K_c \left( \frac{1}{c_1}, a, \alpha_s(\mu) \right). \end{aligned} \quad (65)$$

The primes on the functions  $A'_c$  and  $B'_c$  are to distinguish these anomalous dimensions from their somewhat more familiar versions given below.

The solution to Eq. (62) with  $\mu = \tilde{\mu}_0$  is

$$\begin{aligned} & J_c \left( \frac{p_{J_c} \cdot \hat{\xi}_c}{\tilde{\mu}_0}, \frac{\sqrt{s}}{\tilde{\mu}_0 \nu} (\zeta_c)^{1-a}, a, \alpha_s(\tilde{\mu}_0) \right) = J_c \left( \frac{\sqrt{s}}{2 \zeta_0 \tilde{\mu}_0}, \frac{\sqrt{s}}{\tilde{\mu}_0 \nu} (\zeta_0)^{1-a}, a, \alpha_s(\tilde{\mu}_0) \right) \\ & \times \exp \left\{ - \int_{\sqrt{s}/(2\zeta_0)}^{p_{J_c} \cdot \hat{\xi}_c} \frac{d\lambda}{\lambda} \left[ B'_c(c_1, c_2, a, \alpha_s(c_2\lambda)) + 2 \int_{c_1 \frac{\sqrt{s}^{1-a/2}}{\nu(2\lambda)^{1-a}}}^{c_2\lambda} \frac{d\lambda'}{\lambda'} A'_c(c_1, a, \alpha_s(\lambda')) \right] \right\}, \end{aligned} \quad (66)$$

where we evolve from  $\sqrt{s}/(2\zeta_0)$  to  $p_{J_c} \cdot \hat{\xi}_c = \sqrt{s}/(2\zeta_c)$  (see Eq. (45)) with

$$\zeta_0 = \left( \frac{\nu}{2} \right)^{1/(2-a)}. \quad (67)$$

After combining Eqs. (60) and (66), the choice  $\tilde{\mu}_0 = \sqrt{s}/(2\zeta_0) = \frac{\sqrt{s}}{\nu} (\zeta_0)^{1-a}$  allows us to control

all large logarithms in the jet functions simultaneously:<sup>1</sup>

$$\begin{aligned}
J_c \left( \frac{p_{J_c} \cdot \hat{\xi}_c}{\mu}, \frac{\sqrt{s}}{\mu\nu} (\zeta_c)^{1-a}, a, \alpha_s(\mu) \right) &= J_c \left( 1, 1, a, \alpha_s \left( \frac{\sqrt{s}}{2\zeta_0} \right) \right) \exp \left\{ - \int_{\sqrt{s}/(2\zeta_0)}^{\mu} \frac{d\lambda}{\lambda} \gamma_{J_c}(\alpha_s(\lambda)) \right\} \\
&\times \exp \left\{ - \int_{\sqrt{s}/(2\zeta_0)}^{p_{J_c} \cdot \hat{\xi}_c} \frac{d\lambda}{\lambda} \left[ B'_c(c_1, c_2, a, \alpha_s(c_2\lambda)) + 2 \int_{c_1 \frac{s^{1-a/2}}{\nu(2\lambda)^{1-a}}}^{c_2\lambda} \frac{d\lambda'}{\lambda'} A'_c(c_1, a, \alpha_s(\lambda')) \right] \right\}. \quad (68)
\end{aligned}$$

As observed above, we treat  $a$  as a fixed parameter, with  $|a|$  small compared to  $\ln(1/\varepsilon)$  and  $\ln\nu$ .

### 4.3 The resummed correlation

Using Eq. (68) in (61), and setting  $\mu = \sqrt{s}/2$ , we find a fully resummed form for the correlation,

$$\begin{aligned}
\frac{d\sigma(\varepsilon, \nu, s, a)}{d\varepsilon d\hat{n}_1} &= \frac{d\sigma_0}{d\hat{n}_1} H \left( \frac{2p_{J_c} \cdot \hat{\xi}_c}{\sqrt{s}}, \hat{n}_1, \alpha_s \left( \frac{\sqrt{s}}{2} \right) \right) \\
&\times S \left( 1, \varepsilon\nu, (\zeta_c)^{1-a}, a, \alpha_s(\varepsilon\sqrt{s}) \right) \exp \left\{ - \int_{\varepsilon\sqrt{s}}^{\sqrt{s}/2} \frac{d\lambda}{\lambda} \gamma_s(\alpha_s(\lambda)) \right\} \\
&\times \prod_{c=1}^2 J_c \left( 1, 1, a, \alpha_s \left( \frac{\sqrt{s}}{2\zeta_0} \right) \right) \exp \left\{ - \int_{\sqrt{s}/(2\zeta_0)}^{\sqrt{s}/2} \frac{d\lambda}{\lambda} \gamma_{J_c}(\alpha_s(\lambda)) \right\} \\
&\times \exp \left\{ - \int_{\sqrt{s}/(2\zeta_0)}^{p_{J_c} \cdot \hat{\xi}_c} \frac{d\lambda}{\lambda} \left[ B'_c(c_1, c_2, a, \alpha_s(c_2\lambda)) + 2 \int_{c_1 \frac{s^{1-a/2}}{\nu(2\lambda)^{1-a}}}^{c_2\lambda} \frac{d\lambda'}{\lambda'} A'_c(c_1, a, \alpha_s(\lambda')) \right] \right\}. \quad (69)
\end{aligned}$$

Alternatively, we can combine all jet-related exponents in Eq. (69) in the correlation. As we will verify below in Section 5.2, the cross section is independent of the choice of  $\xi_c$ . As a result, we can choose

$$p_{J_c} \cdot \hat{\xi}_c = \frac{\sqrt{s}}{2}. \quad (70)$$

This choice allows us to combine  $\gamma_{J_c}$  and  $B'_c$  in Eq. (69),

$$\frac{d\sigma(\varepsilon, \nu, s, a)}{d\varepsilon d\hat{n}_1} = \frac{d\sigma_0}{d\hat{n}_1} H \left( 1, \hat{n}_1, \alpha_s \left( \frac{\sqrt{s}}{2} \right) \right)$$

<sup>1</sup>After this paper was submitted for publication, a related analysis of event shape and energy flow correlations was given by Dokshitzer and Marchesini [31], who identify the same factorization of soft radiation described here and in [18], and who study the leading logarithms of  $\varepsilon\nu$  for  $\varepsilon \ll 1/\nu$ , using the methods of [20].



$$\begin{aligned}
& \times S\left(1, \varepsilon\nu, 1, a, \alpha_s(\varepsilon\sqrt{s})\right) \exp\left\{-\int_{\varepsilon\sqrt{s}}^{\sqrt{s}/2} \frac{d\lambda}{\lambda} \gamma_s(\alpha_s(\lambda))\right\} \prod_{c=1}^2 J_c\left(1, 1, a, \alpha_s\left(\frac{\sqrt{s}}{2\zeta_0}\right)\right) \\
& \times \exp\left\{-\int_{\sqrt{s}/(2\zeta_0)}^{\sqrt{s}/2} \frac{d\lambda}{\lambda} \left[\gamma_{J_c}(\alpha_s(\lambda)) + B'_c(c_1, c_2, a, \alpha_s(c_2\lambda)) + 2 \int_{c_1 \frac{s^{1-a/2}}{\nu(2\lambda)^{1-a}}}^{c_2\lambda} \frac{d\lambda'}{\lambda'} A'_c(c_1, a, \alpha_s(\lambda'))\right]\right\},
\end{aligned} \tag{71}$$

with  $\zeta_0$  given by Eq. (67).

In Eqs. (69) and (71), the energy flow  $\varepsilon$  appears at the level of one logarithm per loop, in  $S$ , in the first exponent. Leading logarithms of  $\varepsilon$  are therefore resummed by knowledge of  $\gamma_s^{(1)}$ , the one-loop soft anomalous dimension, where we employ the standard notation,

$$\gamma_s(\alpha_s) = \sum_{n=0}^{\infty} \gamma_s^{(n)} \left(\frac{\alpha_s}{\pi}\right)^n \tag{72}$$

for any expansion in  $\alpha_s$ . At the same time,  $\nu$  appears in up to two logarithms per loop, characteristic of conventional Sudakov resummation. To control  $\nu$ -dependence at the same level as  $\varepsilon$ -dependence, it is natural to work to next-to-leading logarithm in  $\nu$ , by which we mean the level  $\alpha_s^k \ln^k \nu$  in the exponent. As usual, this requires one loop in  $B'_c$  and  $\gamma_{J_c}$ , and two loops in the Sudakov anomalous dimension  $A'_c$ , Eq. (65). These functions are straightforward to calculate from their definitions given in the previous sections. Only the soft function  $S$  in Eqs. (69) and (71) contains information on the geometry of  $\Omega$ . The exponents are partially process-dependent, but geometry-independent. In Section 5, we will derive explicit expressions for these quantities, suitable for resummation to leading logarithm in  $\varepsilon$  and next-to-leading logarithm in  $\nu$ .

## 4.4 The inclusive event shape

It is also of interest to consider the cross section for  $e^+e^-$ -annihilation into two jets without fixing the energy of radiation into  $\Omega$ , but with the final state radiation into all of phase space weighted according to Eq. (4), schematically

$$e^+ + e^- \rightarrow J_1(p_{J_1}, \bar{f}_{\bar{\Omega}_1}) + J_2(p_{J_2}, \bar{f}_{\bar{\Omega}_2}), \tag{73}$$

where  $\bar{\Omega}_1$  and  $\bar{\Omega}_2$  cover the entire sphere. This cross section can be factorized and resummed in a completely analogous manner. The final state is a convolution in the contributions of the jet and soft functions to  $\bar{\varepsilon}$  as in Eq. (27), but with no separate restriction on energy flow into  $\Omega$ . All particles contribute to the event shape. We obtain an expression very analogous to Eq. (69) for this inclusive event shape in transform space, which can be written in terms of the same jet functions as before, and a new function  $S^{\text{incl}}$  for soft radiation as:

$$\frac{d\sigma^{\text{incl}}(\nu, s, a)}{d\hat{n}_1} = \frac{d\sigma_0}{d\hat{n}_1} H\left(\frac{2p_{J_c} \cdot \hat{\xi}_c}{\sqrt{s}}, \hat{n}_1, \alpha_s(\sqrt{s}/2)\right)$$

$$\begin{aligned}
& \times S^{\text{incl}} \left( (\zeta_c)^{1-a}, a, \alpha_s \left( \frac{\sqrt{s}}{\nu} \right) \right) \exp \left\{ - \int_{\sqrt{s}/\nu}^{\sqrt{s}/2} \frac{d\lambda}{\lambda} \gamma_s(\alpha_s(\lambda)) \right\} \\
& \times \prod_{c=1}^2 J_c \left( 1, 1, a, \alpha_s \left( \frac{\sqrt{s}}{2\zeta_0} \right) \right) \exp \left\{ - \int_{\sqrt{s}/(2\zeta_0)}^{\sqrt{s}/2} \frac{d\lambda}{\lambda} \gamma_{J_c}(\alpha_s(\lambda)) \right\} \\
& \times \exp \left\{ - \int_{\sqrt{s}/(2\zeta_0)}^{p_{J_c} \cdot \hat{\xi}_c} \frac{d\lambda}{\lambda} \left[ B'_c(c_1, c_2, a, \alpha_s(c_2\lambda)) + 2 \int_{c_1 \frac{s^{1-a/2}}{\nu(2\lambda)^{1-a}}}^{c_2\lambda} \frac{d\lambda'}{\lambda'} A'_c(c_1, a, \alpha_s(\lambda')) \right] \right\}.
\end{aligned} \tag{74}$$

Here the soft function  $S^{\text{incl}} = 1 + \mathcal{O}(\alpha_s)$ . The double-logarithmic dependence of the shape transform is identical to our resummed correlation, Eq. (69). We will show below, in Sec. 5.3, that Eq. (74) coincides at NLL with the known result for the thrust [6] when we choose  $a = 0$ .

## 5 Results at NLL

### 5.1 Lowest order functions and anomalous dimensions

In this section, we describe the low-order calculations and results that provide explicit expressions for the resummed shape/flow correlations and inclusive event shape distributions at next-to-leading logarithm in  $\nu$  and leading logarithm in  $\varepsilon$  (we refer to this level collectively as NLL below). We go on to verify that for the case  $a = 0$  we rederive the known result for the resummed thrust at NLL, and we exhibit the expressions for the correlation that we will evaluate in Sec. 6.

#### 5.1.1 The soft function

The one-loop soft anomalous dimension is readily calculated in Feynman gauge from the combination of virtual diagrams in  $\sigma^{(\text{eik})}$ , Eq. (48), and  $J^{(\text{eik})}$ , Eq. (49), in Eq. (51). The calculation and the result are equivalent to those of Ref. [14], where the soft function was formulated in axial gauge,

$$\gamma_s^{(1)} = -2 C_F \left[ \sum_{c=1}^2 \ln(\beta_c \cdot \hat{\xi}_c) - \ln \left( \frac{\beta_1 \cdot \beta_2}{2} \right) - 1 \right]. \tag{75}$$

The first,  $\xi_c$ -dependent logarithmic term is associated with the eikonal jets, while the second is a finite remainder from the combination of  $\sigma^{(\text{eik})}$  and  $J^{(\text{eik})}$  in (51). Whenever  $\xi_{c,\perp} = 0$ , the logarithmic terms cancel identically, leaving only the final term, which comes from the  $\hat{\xi}_c$  eikonal self-energy diagrams in the eikonal jet functions.

The soft function is normalized to  $S^{(0)}(\varepsilon) = \delta(\varepsilon)$  as can be seen from (51). For non-zero  $\varepsilon$ ,

$d\sigma/d\varepsilon$  is given at lowest order by

$$S^{(1)}(\varepsilon \neq 0, \Omega) = C_F \frac{1}{\varepsilon} \int_{\Omega} d\text{PS}_2 \frac{1}{2\pi} \frac{\beta_1 \cdot \beta_2}{\beta_1 \cdot \hat{k} \beta_2 \cdot \hat{k}}, \quad (76)$$

where  $\text{PS}_2$  denotes the two-dimensional angular phase space to be integrated over region  $\Omega$ , and  $\hat{k} \equiv k/\omega_k$ . We emphasize again that the soft function contains the only geometry-dependence of the cross section. Also,  $S^{(1)}$  for  $\varepsilon \neq 0$  is independent of  $\nu$  and  $a$ .

As an example, consider a cone with opening angle  $2\delta$ , centered at angle  $\alpha$  from jet 1. In this case, the lowest-order soft function is given by

$$S^{(1)}(\varepsilon \neq 0, \alpha, \delta) = C_F \frac{1}{\varepsilon} \ln \left( \frac{1 - \cos^2 \alpha}{\cos^2 \alpha - \cos^2 \delta} \right). \quad (77)$$

Similarly, we may choose  $\Omega$  as a ring extending angle  $\delta_1$  to the right and  $\delta_2$  to the left of the plane perpendicular to the jet directions in the center-of-mass. In this case, we obtain

$$S^{(1)}(\varepsilon \neq 0, \delta_1, \delta_2) = C_F \frac{1}{\varepsilon} \ln \left( \frac{(1 + \sin \delta_1)(1 + \sin \delta_2)}{(1 - \sin \delta_1)(1 - \sin \delta_2)} \right) = C_F \frac{2}{\varepsilon} \Delta\eta, \quad (78)$$

with  $\Delta\eta$  the rapidity spanned by the ring. For a ring centered around the center-of-mass ( $\delta_1 = \delta_2 = \delta$ ) the angular integral reduces to the form that we encountered in the example of Sec. 2.3, and that we will use in our numerical examples of Sec. 6, with  $\Delta\eta$  given by Eq. (14).

### 5.1.2 The jet functions

Recall from Eq. (39) that the lowest-order jet function is given by  $J_c^{(0)} = 1$ .

The anomalous dimensions of the jet functions are found to be

$$\gamma_{J_c}^{(1)} = -\frac{3}{2} C_F, \quad (79)$$

the same for each of the jets. The jet anomalous dimensions are process-independent, but of course flavor-dependent. The same anomalous dimensions for final-state quark jets appear in three- and higher-jet cross sections.

### 5.1.3 The $K$ - $G$ -decomposition

The anomalous dimension for the  $K$ - $G$ -decomposition is, as noted above, the Sudakov anomalous dimension,

$$\gamma_{K_c}^{(1)} = 2 C_F, \quad (80)$$

$$\gamma_{K_c}^{(2)} = K C_F, \quad (81)$$

also independent of the jet-direction. The well-known coefficient  $K$  (not to be confused with the functions  $K_c$ ) is given by [35]

$$K = \left( \frac{67}{18} - \frac{\pi^2}{6} \right) C_A - \frac{10}{9} T_F N_f, \quad (82)$$

with the normalization  $T_F = 1/2$  and  $N_f$  the number of quark flavors.

$K_c$  and  $G_c$ , the functions that describe the evolution of the jet functions in Eq. (62), are given at one loop by

$$K_c^{(1)} \left( \frac{s^{1-a/2}}{\mu\nu} (2p_{J_c} \cdot \hat{\xi}_c)^{a-1}, a \right) = -C_F \ln \left( e^{2\gamma_E - (1-a)} \frac{\mu^2 \nu^2}{s^{2-a}} (2p_{J_c} \cdot \hat{\xi}_c)^{2(1-a)} \right), \quad (83)$$

$$G_c^{(1)} \left( \frac{p_{J_c} \cdot \hat{\xi}_c}{\mu} \right) = -C_F \ln \left( e^{-1} \frac{(2p_{J_c} \cdot \hat{\xi}_c)^2}{\mu^2} \right). \quad (84)$$

Evolving them to the values of  $\mu$  with which they appear in the functions  $A'_c$  and  $B'_c$ , Eq. (65), they become

$$K_c^{(1)} \left( \frac{1}{c_1}, a \right) = -C_F \ln \left( e^{2\gamma_E - (1-a)} c_1^2 \right), \quad (85)$$

$$G_c^{(1)} \left( \frac{1}{c_2} \right) = -C_F \ln \left( e^{-1} \frac{4}{c_2^2} \right). \quad (86)$$

Recall that  $G_c$  is computed from virtual diagrams only, and thus does not depend on the weight function. It therefore agrees with the result found in [21]. The soft-gluon contribution,  $K_c$ , which involves real gluon diagrams, does depend on the cross section being resummed.

With the definitions (65) of  $A'_c$  and  $B'_c$  we obtain

$$A_c'^{(1)} = C_F, \quad (87)$$

$$A_c'^{(2)}(c_1, a) = \frac{1}{2} C_F \left[ K + \frac{\beta_0}{2} \ln \left( e^{2\gamma_E - 1 + a} c_1^2 \right) \right], \quad (88)$$

$$B_c'^{(1)}(c_1, c_2, a) = 2C_F \ln \left( e^{\gamma_E - 1 + a/2} \frac{2c_1}{c_2} \right). \quad (89)$$

Here  $\beta_0$  is the one-loop coefficient of the QCD beta-function,  $\beta_0 = \frac{1}{3} (11\mathcal{N}_C - 4T_F N_f)$  ( $\beta(g) = -g \frac{\alpha_s}{4\pi} \beta_0 + \mathcal{O}(g^3)$ ).

#### 5.1.4 The hard scattering, and the Born cross section

At NLL only the lowest-order hard scattering function contributes, which is normalized to

$$H^{(0)}(\alpha_s(\sqrt{s}/2)) = 1. \quad (90)$$

At this order the hard function is independent of the eikonal vectors  $\xi_c$ , although it acquires  $\xi_c$ -dependence at higher order through the factorization described in Sec. 3.3. For completeness, we also give the electromagnetic Born cross section  $\frac{d\sigma_0}{d\hat{n}_1}$ , at fixed polar and azimuthal angle:

$$\frac{d\sigma_0}{d\hat{n}_1} = \mathcal{N}_C \left( \sum_f Q_f^2 \right) \frac{\alpha_{\text{em}}^2}{4s} (1 + \cos^2 \theta), \quad (91)$$

where  $\theta$  is the c.m. polar angle of  $\hat{n}_1$ ,  $e Q_f$  is the charge of quark flavor  $f$ , and  $\alpha_{\text{em}} = e^2/(4\pi)$  is the fine structure constant.

## 5.2 Checking the $\xi_c$ -dependence

It is instructive to verify how dependence on the eikonal vectors  $\xi_c$  cancels in the exponents of the resummed cross section (69) at the accuracy at which we work, single logarithms of  $\varepsilon$ , and single and double logarithms of  $\nu$ . In these exponents,  $\xi_c$ -dependence enters only through the combinations  $(\beta_c \cdot \hat{\xi}_c)$  and  $(p_{J_c} \cdot \hat{\xi}_c)$ .

Let us introduce the following notation for the exponents in Eq. (69), to which we will return below:

$$E_1 \equiv - \int_{\varepsilon\sqrt{s}}^{\sqrt{s}/2} \frac{d\lambda}{\lambda} \gamma_s(\alpha_s(\lambda)) - \sum_{c=1}^2 \int_{\sqrt{s}/(2\zeta_0)}^{\sqrt{s}/2} \frac{d\lambda}{\lambda} \gamma_{J_c}(\alpha_s(\lambda)), \quad (92)$$

$$E_2 \equiv - \sum_{c=1}^2 \int_{\sqrt{s}/(2\zeta_0)}^{p_{J_c} \cdot \hat{\xi}_c} \frac{d\lambda}{\lambda} \left[ B'_c(c_1, c_2, a, \alpha_s(c_2\lambda)) + 2 \int_{c_1 \frac{s^{1-a/2}}{\nu(2\lambda)^{1-a}}}^{c_2\lambda} \frac{d\lambda'}{\lambda'} A'_c(c_1, a, \alpha_s(\lambda')) \right]. \quad (93)$$

At NLL, explicit  $\xi_c$  dependence is found only in  $\gamma_s$ , Eq. (75), for  $E_1$ , and in the upper limit of the  $\lambda$  integral of  $E_2$ . We then find that

$$\frac{\partial}{\partial \ln \beta_c \cdot \hat{\xi}_c} (E_1 + E_2) = 2C_F \int_{\varepsilon\sqrt{s}}^{\sqrt{s}/2} \frac{d\lambda}{\lambda} \frac{\alpha_s(\lambda)}{\pi} - 2C_F \int_{c_1 \frac{s^{1-a/2}}{\nu(2p_{J_c} \cdot \hat{\xi}_c)^{1-a}}}^{c_2 p_{J_c} \cdot \hat{\xi}_c} \frac{d\lambda'}{\lambda'} \frac{\alpha_s(\lambda')}{\pi} + \text{NNLL}. \quad (94)$$

Here the second term stems entirely from  $A'^{(1)}$ , Eq. (87); other contributions of  $E_2$  are sub-leading. The  $\xi_c$ -dependence in the exponents begins only at the level that we do not resum, at  $\alpha_s \ln(1/\varepsilon\nu)$ , which is compensated by corrections in  $S(\varepsilon\nu, \alpha_s)$ . The remaining contributions are of NNLL order, that is, proportional to  $\alpha_s^k(\sqrt{s}) \ln^{k-1}(\nu \beta_c \cdot \hat{\xi}_c)$ , as may be verified by expanding the running couplings. Thus, as required by the factorization procedure, the relevant  $\xi_c$ -dependence cancels between the resummed soft and jet functions, which give rise to the first and second integrals, respectively, in Eq. (94).

### 5.3 The inclusive event shape at NLL

We can simplify the differential event shape, Eq. (74), by absorbing the soft anomalous dimension  $\gamma_s$  into the remaining terms. We will find a form that can be compared directly to the classic NLL resummation for the thrust ( $a = 0$ ). This is done by rewriting the integral over the soft anomalous dimension as

$$\begin{aligned}
\int_{\sqrt{s}/\nu}^{\sqrt{s}/2} \frac{d\lambda}{\lambda} \gamma_s(\alpha_s(\lambda)) &= \int_{\sqrt{s}/[2(\nu/2)^{1/(2-a)}]}^{\sqrt{s}/2} \frac{d\lambda}{\lambda} \gamma_s(\alpha_s(\lambda)) + \int_{\sqrt{s}/\nu}^{\sqrt{s}/[2(\nu/2)^{1/(2-a)}]} \frac{d\lambda}{\lambda} \gamma_s(\alpha_s(\lambda)) \\
&= \int_{\sqrt{s}/[2(\nu/2)^{1/(2-a)}]}^{\sqrt{s}/2} \frac{d\lambda}{\lambda} \gamma_s(\alpha_s(\lambda)) + (1-a) \int_{\sqrt{s}/[2(\nu/2)^{1/(2-a)}]}^{\sqrt{s}/2} \frac{d\lambda}{\lambda} \gamma_s\left(\alpha_s\left(\frac{s^{1-a/2}}{\nu(2\lambda)^{1-a}}\right)\right) \\
&= (2-a) \int_{\sqrt{s}/[2(\nu/2)^{1/(2-a)}]}^{\sqrt{s}/2} \frac{d\lambda}{\lambda} \gamma_s(\alpha_s(\lambda)) \\
&\quad - (1-a) \int_{\sqrt{s}/[2(\nu/2)^{1/(2-a)}]}^{\sqrt{s}/2} \frac{d\lambda}{\lambda} \int_{s^{1-a/2}/[\nu(2\lambda)^{1-a}]}^{\lambda} \frac{d\lambda'}{\lambda'} \beta(g(\lambda')) \frac{\partial}{\partial g} \gamma_s(\alpha_s(\lambda')). \quad (95)
\end{aligned}$$

In the first equality we split the  $\lambda$  integral so that the limits of the first term match those of the  $B'_c$  integral of Eq. (74). In the second equality we have changed variables in the second term according to

$$\lambda \rightarrow \left( \frac{s^{1-a/2}}{2^{1-a}\nu\lambda} \right)^{\frac{1}{1-a}}, \quad (96)$$

so that the limits of the second integral also match. In the third equality of Eq. (95), we have reexpressed the running coupling at the old scale  $\lambda$  in terms of the new scale. This is a generalization of the procedure of Ref. [36], applied originally to the threshold-resummed Drell-Yan cross section [37].

Using Eq. (95), and identifying  $p_{J_c} \cdot \hat{\xi}_c$  with  $\sqrt{s}/2$  (Eq. (70)) in the inclusive event shape distribution, Eq. (74), we can rewrite this distribution at NLL as

$$\begin{aligned}
\frac{d\sigma^{\text{incl}}(\nu, s, a)}{d\hat{n}_1} &= \frac{d\sigma_0}{d\hat{n}_1} \\
&\times \prod_{c=1}^2 \exp \left\{ - \int_{\sqrt{s}/[2(\nu/2)^{1/(2-a)}]}^{\sqrt{s}/2} \frac{d\lambda}{\lambda} \left[ B_c(c_1, c_2, a, \alpha_s(\lambda)) + 2 \int_{c_1 \frac{s^{1-a/2}}{\nu(2\lambda)^{1-a}}}^{c_2 \lambda} \frac{d\lambda'}{\lambda'} A_c(c_1, a, \alpha_s(\lambda')) \right] \right\}, \quad (97)
\end{aligned}$$

where we have rearranged the contribution of  $\gamma_s$  as:

$$\begin{aligned}
A_c(c_1, a, \alpha_s(\mu)) &\equiv A'_c(c_1, a, \alpha_s(\mu)) - \frac{1}{4}(1-a)\beta(g(\mu)) \frac{\partial}{\partial g} \gamma_s(\alpha_s(\mu)), \\
B_c(c_1, c_2, a, \alpha_s(\mu)) &\equiv \gamma_{J_c}(\alpha_s(\mu)) + \left(1 - \frac{a}{2}\right) \gamma_s(\alpha_s(\mu)) + B'_c(c_1, c_2, a, \alpha_s(\mu)). \quad (98)
\end{aligned}$$

Next, we replace the lower limit of the  $\lambda'$ -integral by an explicit  $\theta$ -function. Then we exchange orders of integration, and change variables in the term containing  $A$  from the dimensionful variable  $\lambda$  to the dimensionless combination

$$u = \frac{2\lambda\lambda'}{s}. \quad (99)$$

We find

$$\begin{aligned} \frac{d\sigma^{\text{incl}}(\nu, s, a)}{d\hat{n}_1} &= \frac{d\sigma_0}{d\hat{n}_1} \prod_{c=1}^2 \exp \left\{ - \int_{\sqrt{s}/[2(\nu/2)^{1/(2-a)}}^{\sqrt{s}/2} \frac{d\lambda}{\lambda} B_c(c_1, c_2, a, \alpha_s(\lambda)) \right\} \\ &\times \prod_{c=1}^2 \exp \left\{ -2 \int_0^{\sqrt{s}} \frac{d\lambda'}{\lambda'} \int_{\lambda'^2/s}^{\lambda'/\sqrt{s}} \frac{du}{u} \theta \left( c_1^{-1} \nu \frac{\lambda'^a u^{1-a}}{s^{a/2}} - 1 \right) A_c(c_1, a, \alpha_s(\lambda')) \right\}. \end{aligned} \quad (100)$$

Here, the  $\theta$ -function vanishes for small  $\lambda'$ , and the remaining effects of replacing the lower boundary of the  $\lambda'$  integral by 0 are next-to-next-to-leading logarithmic.

A further change of variables allows us to write the NLL resummed event shapes in a form familiar from the NLL resummed thrust. In the first line of Eq. (100), we replace  $\lambda^2 \rightarrow us/4$ . In the second line we relabel  $\lambda' \rightarrow \sqrt{q^2}$ , and exchange orders of integration. Finally, choosing

$$\begin{aligned} c_1 &= e^{-\gamma_E}, \\ c_2 &= 2, \end{aligned} \quad (101)$$

we find at NLL

$$\begin{aligned} \frac{d\sigma^{\text{incl}}(\nu, s, a)}{d\hat{n}_1} &= \frac{d\sigma_0}{d\hat{n}_1} \prod_{c=1}^2 \exp \left\{ \int_0^1 \frac{du}{u} \left[ \int_{u^2 s}^{us} \frac{dq^2}{q^2} A_c(\alpha_s(q^2)) \left( e^{-u^{1-a} \nu (q^2/s)^{a/2}} - 1 \right) \right. \right. \\ &\quad \left. \left. + \frac{1}{2} B_c(\alpha_s(us/4)) \left( e^{-u(\nu/2)^{2/(2-a)} e^{-\gamma_E}} - 1 \right) \right] \right\}, \end{aligned} \quad (102)$$

and reproduce the well-known coefficients

$$A_c^{(1)} = C_F, \quad (103)$$

$$A_c^{(2)} = \frac{1}{2} C_F K, \quad (104)$$

$$B_c^{(1)} = -\frac{3}{2} C_F, \quad (105)$$

independent of  $a$ . In Eq. (102), we have made use of the relation

$$e^{-x/y} - 1 \approx -\theta(x - y e^{-\gamma_E}), \quad (106)$$

which is valid at NLL in the logarithmic integrals. With these choices, when  $a = 0$  we reproduce the NLL resummed thrust cross section [6].

The choices of the  $c_i$  in Eq. (101) cancel all purely soft NLL components ( $\gamma_s$  and  $K_c$ ). The remaining double logarithms stem from simultaneously soft and collinear radiation, and single logarithms arise from collinear configurations only. At NLL, the cross section is determined by the anomalous dimension  $A_c$ , which is the coefficient of the singular  $1/[1-x]_+$  term in the nonsinglet evolution kernel [38], and the quark anomalous dimension. All radiation in dijet events thus appears to be emitted coherently by the two jets [6]. This, however, is not necessarily true beyond next-to-leading logarithmic accuracy for dijets, and is certainly not the case for multijet events [14]. Similar considerations apply to the resummed correlation, Eq. (69).

## 5.4 Closed expressions

Given the explicit results above, the integrals in the exponents of the resummed correlation, Eq. (69), may be easily performed in closed form. We give the analytic results for the exponents of Eq. (69), as defined in Eqs. (92) and (93). As in Eq. (70), we identify  $p_{J_c} \cdot \hat{\xi}_c$  with  $\sqrt{s}/2$ .

$$e^{E_1(a)} = \left( \frac{\alpha_s(\sqrt{s}/2)}{\alpha_s(\varepsilon\sqrt{s})} \right)^{\frac{4C_F}{\beta_0}} \left( \frac{\alpha_s\left(\frac{\sqrt{s}}{2\zeta_0}\right)}{\alpha_s(\sqrt{s}/2)} \right)^{\frac{6C_F}{\beta_0}}, \quad (107)$$

$$e^{E_2(a)} = \left( \frac{\alpha_s(c_2\sqrt{s}/2)}{\alpha_s\left(\frac{c_2\sqrt{s}}{2\zeta_0}\right)} \right)^{\frac{4C_F}{\beta_0}\kappa_1(a)} \left( \frac{\alpha_s\left(\frac{c_1\sqrt{s}}{2\zeta_0}\right)}{\alpha_s\left(\frac{c_1\sqrt{s}}{\nu}\right)} \right)^{\frac{1}{a-1}\frac{4C_F}{\beta_0}\kappa_2(a)} \left( \frac{\alpha_s(c_2\sqrt{s}/2)}{\alpha_s\left(\frac{c_1\sqrt{s}}{2\zeta_0}\right)} \right)^{\frac{1}{2-a}\frac{8C_F}{\beta_0}\ln(\nu/2)}, \quad (108)$$

with

$$\kappa_1(a) = \ln\left(\frac{4}{c_2^2 e}\right) + \frac{4\pi}{\beta_0} \left[ \alpha_s\left(\frac{c_2\sqrt{s}}{2\zeta_0}\right) \right]^{-1} - \frac{2K}{\beta_0} - \frac{\beta_1}{2\beta_0^2} \ln\left(\left(\frac{\beta_0}{4\pi e}\right)^2 \alpha_s\left(\frac{c_2\sqrt{s}}{2}\right) \alpha_s\left(\frac{c_2\sqrt{s}}{2\zeta_0}\right)\right), \quad (109)$$

$$\kappa_2(a) = (1-a-2\gamma_E) + \frac{4\pi}{\beta_0} \left[ \alpha_s\left(\frac{\sqrt{s}}{\nu}\right) \right]^{-1} - \frac{2K}{\beta_0} - \frac{\beta_1}{2\beta_0^2} \ln\left(\left(\frac{\beta_0}{4\pi e}\right)^2 \alpha_s\left(\frac{c_1\sqrt{s}}{\nu}\right) \alpha_s\left(\frac{c_1\sqrt{s}}{2\zeta_0}\right)\right). \quad (110)$$

We have used the two-loop running coupling, when appropriate, to derive Eqs. (107) - (110). The results are expressed in terms of the one-loop running coupling

$$\alpha_s(\mu) = \frac{2\pi}{\beta_0} \frac{1}{\ln\left(\frac{\mu}{\Lambda_{\text{QCD}}}\right)}, \quad (111)$$

and the first two coefficients in the expansion of the QCD beta-function,  $\beta_0$  and

$$\beta_1 = \frac{34}{3} C_A^2 - \left(\frac{20}{3} C_A + 4C_F\right) T_F N_f. \quad (112)$$



Combining the expressions for the exponents, Eqs. (107) and (108), for the Born cross section, Eq. (91), and for the soft function, Eq. (76), in Eq. (69), the complete differential cross section, at LL in  $\varepsilon$  and at NLL in  $\nu$ , is given by

$$\begin{aligned}
\frac{d\sigma(\varepsilon, \nu, s, a)}{d\varepsilon d\hat{n}_1} &= \mathcal{N}_C \left( \sum_f Q_f^2 \right) \frac{\pi\alpha_{\text{em}}^2}{2s} (1 + \cos^2\theta) C_F \frac{\alpha_s(\varepsilon\sqrt{s})}{\pi} \frac{1}{\varepsilon} \int_{\Omega} d\text{PS}_2 \frac{1}{2\pi} \frac{\beta_1 \cdot \beta_2}{\beta_1 \cdot \hat{k} \beta_2 \cdot \hat{k}} \\
&\times \left( \frac{\alpha_s\left(\frac{\sqrt{s}}{2}\right)}{\alpha_s(\varepsilon\sqrt{s})} \right)^{\frac{4C_F}{\beta_0}} \left( \frac{\alpha_s\left(\frac{\sqrt{s}}{2\zeta_0}\right)}{\alpha_s\left(\frac{\sqrt{s}}{2}\right)} \right)^{\frac{6C_F}{\beta_0}} \\
&\times \left( \frac{\alpha_s\left(c_2\frac{\sqrt{s}}{2}\right)}{\alpha_s\left(\frac{c_2\sqrt{s}}{2\zeta_0}\right)} \right)^{\frac{4C_F}{\beta_0}\kappa_1(a)} \left( \frac{\alpha_s\left(\frac{c_1\sqrt{s}}{2\zeta_0}\right)}{\alpha_s\left(\frac{c_1\sqrt{s}}{\nu}\right)} \right)^{\frac{1}{a-1}\frac{4C_F}{\beta_0}\kappa_2(a)} \left( \frac{\alpha_s\left(c_2\frac{\sqrt{s}}{2}\right)}{\alpha_s\left(\frac{c_1\sqrt{s}}{2\zeta_0}\right)} \right)^{\frac{1}{2-a}\frac{8C_F}{\beta_0} \ln\left(\frac{\nu}{2}\right)}. \quad (113)
\end{aligned}$$

These are the expressions that we will evaluate in the next section. We note that this is not the only possible closed form for the resummed correlation at this level of accuracy. When a full next-to-leading order calculation for this set of event shapes is given, the matching procedure of [6] may be more convenient.

## 6 Numerical Results

Here we show some representative examples of numerical results for the correlation, Eq. (113). We pick the constants  $c_i$  as in Eq. (101), unless stated otherwise. The effect of different choices is nonleading, and is numerically small, as we will see below. In the following we choose the region  $\Omega$  to be a ring between the jets, centered in their center-of-mass, with a width of  $\Delta\eta = 2$ , or equivalently, opening angle  $\delta \approx 50$  degrees (see Eq. (14)). The analogous cross section for a cone centered at 90 degrees from the jets (Eq. (77)) has a similar behavior. In the following, the center-of-mass energy  $Q = \sqrt{s}$  is chosen to be 100 GeV.

Fig. 5 shows the dependence of the differential cross section (69), multiplied by  $\varepsilon$  and normalized by the Born cross section,  $\frac{\varepsilon d\sigma/(d\varepsilon d\hat{n}_1)}{d\sigma_0/d\hat{n}_1}$ , on the measured energy  $\varepsilon$  and on the parameter  $a$ , at fixed  $\nu$ . In Fig. 5 a), we plot  $\frac{\varepsilon d\sigma/(d\varepsilon d\hat{n}_1)}{d\sigma_0/d\hat{n}_1}$  for  $\nu = 10$ , in Fig. 5 b) for  $\nu = 50$ . As  $\nu$  increases, the radiation into the complementary region  $\bar{\Omega}$  is more restricted, as illustrated by the comparison of Figs. 5 a) and b). Similarly, as  $a$  approaches 1, the cross section falls, because the jets are restricted to be very narrow. On the other hand, as  $a$  assumes more and more negative values at fixed  $\varepsilon$ , the correlations (69) approach a constant value. For  $a$  large and negative, however, non-global dependence on  $\ln\varepsilon$  and  $|a|$  will emerge from higher order corrections in the soft function, which we do not include in Eq. (113).

In Fig. 6 we investigate the sensitivity of the resummed correlation, Eq. (113), to our choice of the constants  $c_i$ . The effect of these constants is of next-to-next-to-leading logarithmic order in the event shape. We plot the differential cross section  $\varepsilon \frac{d\sigma/(d\varepsilon d\hat{n}_1)}{d\sigma_0/d\hat{n}_1}$ , at  $Q = 100$  GeV, for fixed  $\varepsilon = 0.05$  and  $\nu = 20$ , as a function of  $a$ . The effects of changes in the  $c_i$  are of the order of a few percent for moderate values of  $a$ .

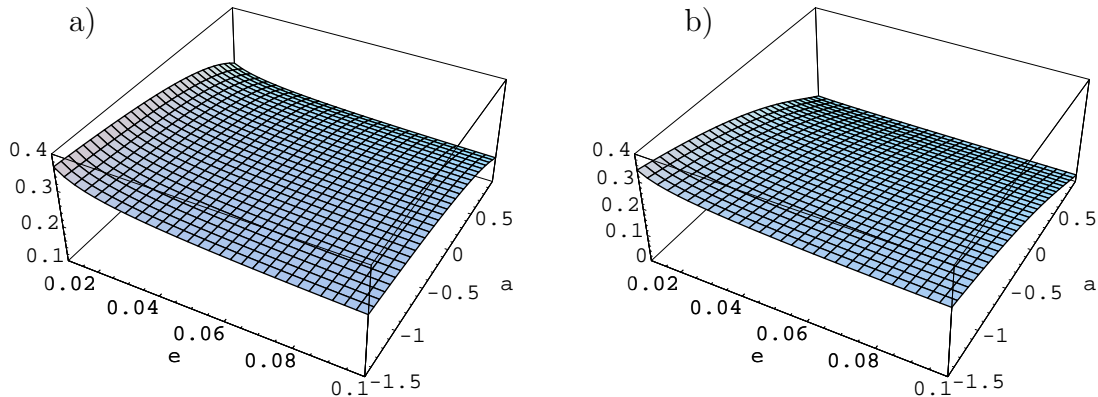


Figure 5: Differential cross section  $\frac{\varepsilon d\sigma/(d\varepsilon d\hat{n}_1)}{d\sigma_0/d\hat{n}_1}$ , normalized by the Born cross section, at  $Q = 100$  GeV, as a function of  $\varepsilon$  and  $a$  at fixed  $\nu$ : a)  $\nu = 10$ , b)  $\nu = 50$ .  $\Omega$  is a ring (slice) centered around the jets, with a width of  $\Delta\eta = 2$ .

Finally, we illustrate the sensitivity of these results to the flavor of the primary partons. For this purpose we study the corresponding ratio of the shape/flow correlation to the cross section for gluon jets produced by a hypothetical color singlet source. Fig. 7 displays the ratio of the differential cross section  $d\sigma^a(\varepsilon, a)/(d\varepsilon d\hat{n}_1)$ , Eq. (113), normalized by the lowest-order cross section, to the analogous quantity with gluons as primary partons in the outgoing jets, again at  $Q = 100$  GeV. This ratio is multiplied by  $C_A/C_F$  in the figure to compensate for the difference in the normalizations of the lowest-order soft functions. Gluon jets have wider angular extent, and hence are suppressed relative to quark jets with increasing  $\nu$  or  $a$ , as can be seen by comparing Figs. 7 a) and b). Fig. 7 a) shows the ratio at  $\nu = 10$ , and Fig. 7 b) at  $\nu = 50$ . These results suggest sensitivity to the more complex color and flavor flow characteristic of hadronic scattering [14, 15].

## 7 Summary and Outlook

We have introduced a general class of inclusive event shapes in  $e^+e^-$  dijet events which reduce to the thrust and the jet broadening distributions as special cases. We have derived analytic expressions in transform space, and have shown the equivalence of our formalism at NLL with the well-known result for the thrust [6]. Separate studies of this class of event shapes in the untransformed space, at higher orders, and for nonperturbative effects [9] are certainly of interest. We reserve these studies for future work.

We have introduced a set of correlations of interjet energy flow for the general class of event shapes, and have shown that for these quantities it is possible to control the influence of secondary radiation and nonglobal logarithms. These correlations are sensitive mainly to radiation

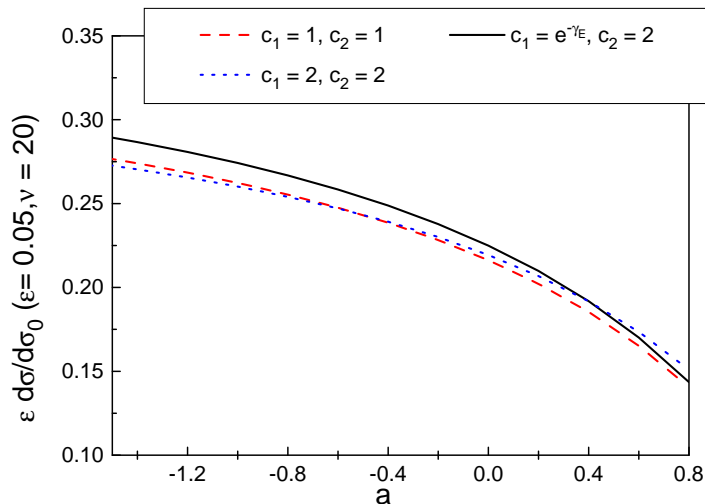


Figure 6: Differential cross section  $\frac{\varepsilon d\sigma/(d\varepsilon d\hat{n}_1)}{d\sigma_0/d\hat{n}_1}$ , normalized by the Born cross section, at  $Q = 100$  GeV, as a function of  $a$  at fixed  $\nu = 20$  and  $\varepsilon = 0.05$ .  $\Omega$  is chosen as in Fig. 5. Solid line:  $c_1 = e^{-\gamma E}$ ,  $c_2 = 2$ , as in Eq. (101), dashed line:  $c_1 = c_2 = 1$ , dotted line:  $c_1 = c_2 = 2$ .

emitted directly from the primary hard scattering, through transforms in the weight functions that suppress secondary, or non-global, radiation. We have presented analytic and numerical studies of these shape/flow correlations at leading logarithmic order in the flow variable and at next-to-leading-logarithmic order in the event shape. The application of our formalism to multi-jet events and to scattering with initial state hadrons is certainly possible, and may shed light on the relationship between color and energy flow in hard scattering processes with non-trivial color exchange.

## Acknowledgements

We thank Maria Elena Tejeda-Yeomans for many helpful discussions, and Gavin Salam for useful conversations. This work was supported in part by the National Science Foundation grant PHY0098527.

## A Eikonal Example

In this appendix, we give details of the calculation of the logarithmic behavior in the diagrams of Fig. 3. We choose the reference frame such that the momenta of the final state particles are given by:

$$\beta_1 = (1, 0, 0, 1),$$

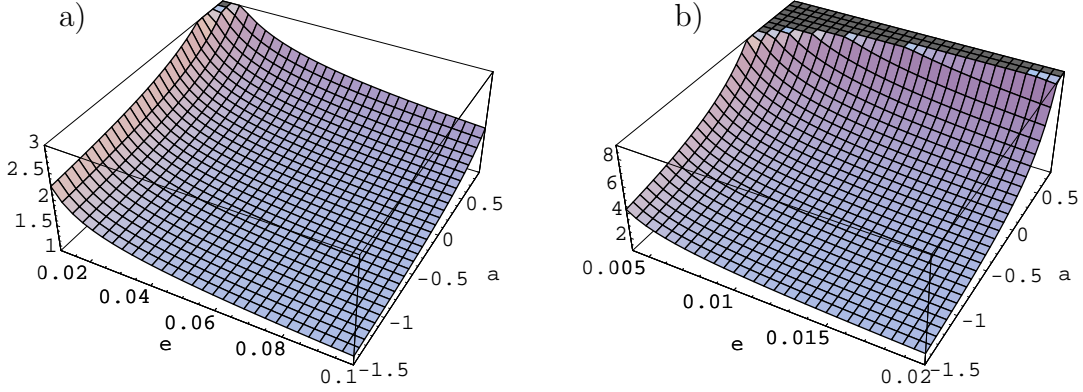


Figure 7: Ratios of differential cross sections for quark to gluon jets  $\frac{C_A}{C_F} \left( \frac{\varepsilon d\sigma^q/(d\varepsilon d\hat{n}_1)}{d\sigma_0^q/d\hat{n}_1} \right) \left( \frac{\varepsilon d\sigma^g/(d\varepsilon d\hat{n}_1)}{d\sigma_0^g/d\hat{n}_1} \right)^{-1}$  at  $Q = 100$  GeV as a function of  $\varepsilon$  and  $a$  at fixed  $\nu$ : a)  $\nu = 10$ , b)  $\nu = 50$ .  $\Omega$  as in Fig. 5,  $c_1$  and  $c_2$  as in Eq. (101).

$$\begin{aligned}
\beta_2 &= (1, 0, 0, -1), \\
l &= \omega_l(1, s_l, 0, c_l), \\
k &= \omega_k(1, s_k \cos \phi, s_k \sin \phi, c_k).
\end{aligned} \tag{114}$$

Here we define  $s_{l,k} \equiv \sin \theta_{l,k}$  and  $c_{l,k} \equiv \cos \theta_{l,k}$ .  $\theta_l$  is the angle between the vectors  $\vec{l}$  and  $\vec{\beta}_1$ ,  $\theta_k$  is the angle between the vectors  $\vec{k}$  and  $\vec{\beta}_1$  and  $\phi$  is the azimuthal angle of the gluon with momentum  $k$  relative to the plane defined by  $\beta_1$ ,  $\beta_2$  and  $l$ . The available phase space in polar angle for the radiated gluons is  $\theta_k \in (\pi/2 - \delta, \pi/2 + \delta)$  and  $\theta_l \in (0, \pi/2 - \delta) \cup (\pi/2 + \delta, \pi)$ .

Using the diagrammatic rules for eikonal lines and vertices, as listed for example in [26], we can write down the expressions corresponding to each diagram separately. For example, diagram 3 a) gives

$$\begin{aligned}
a) + (k \leftrightarrow l) &= [f_{abc} \text{Tr}(t_a t_b t_c)] \left( -ig_s^4 \beta_1^\alpha \beta_2^\beta \beta_1^\gamma \right) V_{\alpha\beta\gamma}(k+l, -k, -l) \frac{1}{\beta_1 \cdot (k+l)} \frac{1}{2k \cdot l} \frac{1}{\beta_1 \cdot l} \frac{1}{\beta_2 \cdot k} \\
&+ (k \leftrightarrow l).
\end{aligned} \tag{115}$$

$V_{\alpha\beta\gamma}(k+l, -k, -l) = [(2k+l)_\gamma g_{\alpha\beta} + (l-k)_\alpha g_{\beta\gamma} - (2l+k)_\beta g_{\alpha\gamma}]$  is the momentum-dependent part of the three gluon vertex. Using the color identity  $f_{abc} \text{Tr}(t_a t_b t_c) = iC_F \mathcal{N}_C C_A/2$ , and the approximation  $\beta_j \cdot l \gg \beta_j \cdot k$  for  $j = 1, 2$ , which is valid due to the strong ordering of the final state gluon energies, we arrive at

$$a) + (k \leftrightarrow l) = \frac{1}{4} C_F \mathcal{N}_C C_A g_s^4 \frac{\beta_1 \cdot \beta_2}{k \cdot l} \left( \frac{1}{\beta_1 \cdot k \beta_2 \cdot l} + \frac{2}{\beta_1 \cdot l \beta_2 \cdot k} \right). \tag{116}$$

We proceed in a similar manner for the rest of the diagrams. The results are:

$$\begin{aligned}
b) + (k \leftrightarrow l) &= \frac{1}{4} C_F \mathcal{N}_C C_A g_s^4 \frac{\beta_1 \cdot \beta_2}{k \cdot l} \left( \frac{2}{\beta_1 \cdot k \beta_2 \cdot l} + \frac{1}{\beta_1 \cdot l \beta_2 \cdot k} \right), \\
c) &= \frac{1}{4} C_F \mathcal{N}_C C_A g_s^4 \frac{\beta_1 \cdot \beta_2}{k \cdot l} \frac{1}{\beta_1 \cdot l} \frac{1}{\beta_2 \cdot k}, \\
d) &= \frac{1}{4} C_F \mathcal{N}_C C_A g_s^4 \frac{\beta_1 \cdot \beta_2}{k \cdot l} \frac{1}{\beta_1 \cdot k} \frac{1}{\beta_2 \cdot l}, \\
e) &= C_F \mathcal{N}_C (C_F - C_A/2) g_s^4 \frac{(\beta_1 \cdot \beta_2)^2}{\beta_1 \cdot l \beta_2 \cdot l} \frac{1}{\beta_1 \cdot k \beta_2 \cdot k}, \\
f) + (k \leftrightarrow l) &= C_F \mathcal{N}_C (C_F - C_A/2) g_s^4 \frac{(\beta_1 \cdot \beta_2)^2}{\beta_1 \cdot l \beta_2 \cdot l} \frac{2}{\beta_1 \cdot k \beta_2 \cdot k}. \tag{117}
\end{aligned}$$

The color factors in the last two equations of (117) are obtained from the identity  $\text{Tr}(t_a t_b t_a t_b) = C_F \mathcal{N}_C (C_F - C_A/2)$ . Combining the terms proportional to the color factor  $C_F \mathcal{N}_C C_A$ , and including the complex conjugate diagrams, we find for the squared amplitude

$$|M|^2 = 2 g_s^4 C_F \mathcal{N}_C C_A \beta_1 \cdot \beta_2 \left( \frac{1}{k \cdot l \beta_1 \cdot k \beta_2 \cdot l} + \frac{1}{k \cdot l \beta_1 \cdot l \beta_2 \cdot k} - \frac{\beta_1 \cdot \beta_2}{\beta_1 \cdot l \beta_2 \cdot l \beta_1 \cdot k \beta_2 \cdot k} \right). \tag{118}$$

Having determined the amplitude, we need to integrate  $|M|^2$  over the phase space corresponding to the geometry given in Fig. 2. Specifically, we have to evaluate:

$$I \equiv \frac{1}{\mathcal{N}_C} \int d\bar{\varepsilon} e^{-\nu \bar{\varepsilon}} \int_{\Omega} \frac{d^3 k}{(2\pi)^3 2\omega_k} \int_{\bar{\Omega}} \frac{d^3 l}{(2\pi)^3 2\omega_l} \delta(\varepsilon - \omega_k/\sqrt{s}) \delta(\bar{\varepsilon} - \bar{f}(l, a)) |M|^2, \tag{119}$$

where the weight function  $\bar{f}(l, a)$  is given, as in Eqs. (4) and (11), by

$$\bar{f}(l, a) = \begin{cases} \frac{\omega_l}{\sqrt{s}} (1 - c_l)^{1-a} s_l^a & : \theta_l \in (0, \pi/2 - \delta) \\ \frac{\omega_l}{\sqrt{s}} (1 + c_l)^{1-a} s_l^a & : \theta_l \in (\pi/2 + \delta, \pi), \end{cases} \tag{120}$$

with  $a < 1$ .

Using the equalities:  $\beta_1 \cdot \beta_2 = 2$ ,  $\beta_1 \cdot l = \omega_l(1 - c_l)$ ,  $\beta_2 \cdot l = \omega_l(1 + c_l)$ ,  $\beta_1 \cdot k = \omega_k(1 - c_k)$ ,  $\beta_2 \cdot k = \omega_k(1 + c_k)$  and  $k \cdot l = \omega_k \omega_l (1 - c_k c_l - s_k s_l \cos \phi)$  in Eq. (118), performing the integration over  $\phi$ , and changing the integration variable  $c_l \rightarrow -c_l$  in the angular region  $\theta_l \in (\pi/2 + \delta, \pi)$ , we easily arrive at the following three-dimensional integral:

$$\begin{aligned}
I &= C_F C_A \left( \frac{\alpha_s}{\pi} \right)^2 \frac{1}{\varepsilon} \int_{-\sin \delta}^{\sin \delta} dc_k \int_{\sin \delta}^1 dc_l \int_{\varepsilon/\sqrt{s}}^{\sqrt{s}} \frac{d\omega_l}{\omega_l} e^{-\nu \omega_l (1-c_l)^{1-a} s_l^a / \sqrt{s}} \\
&\quad \left[ \frac{1}{c_k + c_l} \frac{1}{1 + c_k} \left( \frac{1}{1 + c_l} + \frac{1}{1 - c_k} \right) - \frac{1}{s_k^2} \frac{1}{1 + c_l} \right]. \tag{121}
\end{aligned}$$

We are interested in the  $(1/\varepsilon) \ln(1/\varepsilon)$  behavior of  $I$ . This is obtained after performing the  $\omega_l$  integral with the replacement  $e^{-\nu \omega_l (1-c_l)^{1-a} s_l^a / \sqrt{s}} \rightarrow \theta(1 - \nu \omega_l (1 - c_l)^{1-a} s_l^a / \sqrt{s})$ . Remainders do

not contain terms proportional to  $\ln \varepsilon$ . In this approximation, the  $c_l$  integration can be carried out, and we obtain the integral representation for the term containing  $(1/\varepsilon) \ln(1/\varepsilon)$ :

$$I = 2 C_F C_A \left( \frac{\alpha_s}{\pi} \right)^2 \frac{1}{\varepsilon} \ln \left( \frac{1}{\varepsilon \nu} \right) \left[ \int_0^{\sin \delta} \frac{dc_k}{s_k^2} \ln \left( \frac{s_k^2}{s_k^2 - \cos^2 \delta} \right) - \ln \left( \frac{2}{1 + \sin \delta} \right) \ln \left( \frac{1 + \sin \delta}{1 - \sin \delta} \right) \right]. \quad (122)$$

The potential non-global logarithm of  $\varepsilon$  is replaced by  $\ln(\varepsilon \nu)$ . The angular integral over  $c_k$  can be expressed in terms of dilogarithmic functions. The final expression for the term proportional to  $\ln(\varepsilon \nu)/\varepsilon$  takes the form:

$$I = C_F C_A \left( \frac{\alpha_s}{\pi} \right)^2 \frac{1}{\varepsilon} \ln \left( \frac{1}{\varepsilon \nu} \right) \left[ \frac{\pi^2}{6} + \ln \left( \frac{\cot \delta (1 + \sin \delta)}{4} \right) \ln \left( \frac{1 + \sin \delta}{1 - \sin \delta} \right) + \text{Li}_2 \left( \frac{1 - \sin \delta}{2} \right) - \text{Li}_2 \left( \frac{1 + \sin \delta}{2} \right) - \text{Li}_2 \left( -\frac{2 \sin \delta}{1 - \sin \delta} \right) - \text{Li}_2 \left( \frac{1 - \sin \delta}{1 + \sin \delta} \right) \right]. \quad (123)$$

Equivalently, we can express our results in terms of the rapidity width of the region  $\Omega$ , Eq. (14), and we obtain

$$I = C_F C_A \left( \frac{\alpha_s}{\pi} \right)^2 \frac{1}{\varepsilon} \ln \left( \frac{1}{\varepsilon \nu} \right) \left[ \frac{\pi^2}{6} + \Delta \eta \left( \frac{\Delta \eta}{2} - \ln(2 \sinh(\Delta \eta)) \right) + \text{Li}_2 \left( \frac{e^{-\Delta \eta/2}}{2 \cosh(\Delta \eta/2)} \right) - \text{Li}_2 \left( \frac{e^{\Delta \eta/2}}{2 \cosh(\Delta \eta/2)} \right) - \text{Li}_2 \left( -2 \sinh(\Delta \eta/2) e^{\Delta \eta/2} \right) - \text{Li}_2(e^{-\Delta \eta}) \right]. \quad (124)$$

The coefficient

$$C(\Delta \eta) \equiv - \left( \frac{\pi}{\alpha_s} \right)^2 \frac{\varepsilon I}{C_F C_A \ln(\varepsilon \nu)} \quad (125)$$

as a function of  $\Delta \eta$  is shown in Fig. 8. Naturally,  $C$  is a monotonically increasing function of  $\Delta \eta$ . For  $\Delta \eta \rightarrow 0$ ,

$$C \sim \mathcal{O}(\Delta \eta \ln \Delta \eta), \quad (126)$$

and the cross section vanishes, as expected. On the other hand, as the size of region  $\Omega$  increases,  $C$  rapidly saturates and reaches its limiting value [17]

$$\lim_{\Delta \eta \rightarrow \infty} C = \frac{\pi^2}{6}. \quad (127)$$

## B Recoil

In this appendix, we return to the justification of the technical step represented by Eq. (23). According to this approximation, we may compute the jet functions by identifying axes that depend only upon particles in the final states  $N_{J_c}$  associated with those functions, rather than the full final state  $N$ . Intuitively, this is a reasonable estimate, given that the jet axis should be

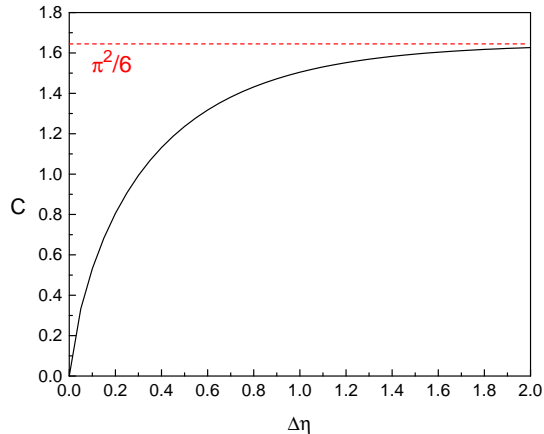


Figure 8:  $C(\Delta\eta)$ , as defined in (125), as a function of rapidity width  $\Delta\eta$  of the region  $\Omega$ . The dashed line is its limiting value,  $C(\Delta\eta \rightarrow \infty) = \pi^2/6$ .

determined by a set of energetic, nearly collinear particles. When we make this replacement, however, the contributions to the event shape from energetic particles near the jet axis may change. This change is neglected in going from the original factorization, Eq. (21), to the factorization in convolution form, Eq. (27), which is the starting point for the resummation techniques that we employ in this paper. The weight functions  $\bar{f}^N(N_i, a)$  in Eq. (21) are defined relative to the unit vector  $\hat{n}_1$  corresponding to  $a = 0$ , the thrust-like event shape. The factorization of Eq. (21) applies to any  $a < 2$ , but as indicated by the superscript, individual contributions to  $\bar{f}^N(N_i, a)$  on the right-hand side continue to depend on the full final state  $N$ , through the identification of the jet axis.

To derive the factorization of Eq. (27) in a simple convolution form, we must be able to treat the thrust axis,  $\hat{n}_1$ , as a fixed vector for each of the states  $N_s, N_{J_c}$ . This is possible if we can neglect the effects of recoil from soft, wide-angle radiation on the direction of the axis. Specifically, we must be able to make the replacement

$$\bar{f}_{\Omega_c}^N(N_{J_c}, a) \rightarrow \bar{f}_c(N_{J_c}, a), \quad (128)$$

where  $\bar{f}_c(N_{J_c}, a)$  is the event shape variable for jet  $c$ , in which the axis  $\hat{n}_c$  is specified by state  $N_{J_c}$  *only*. Of course, this replacement changes the value of the weight,  $\bar{\varepsilon}, \bar{f}_{\Omega_c}^N(N_{J_c}, a) \neq \bar{f}_c(N_{J_c}, a)$ . As we now show, the error induced by this replacement is suppressed by a power of  $\bar{\varepsilon}$  so long as  $a < 1$ . In general, the error is nonnegligible for  $a \geq 1$ . The importance of recoil for jet broadening, at  $a = 1$ , was pointed out in [8]. We now discuss how the neglect of such radiation affects the jet axis (always determined from  $a = 0$ ) and hence the value of the event shape for arbitrary  $a < 2$ .

The jet axis is found by minimizing  $\bar{f}(a = 0)$  in each state. The largest influence on the axis  $\hat{n}_c$  for jet  $c$  is, of course, the set of fast, collinear particles within the state  $N_{J_c}$  associated with the jet function in Eq. (21). Soft, wide-angle radiation, however, does affect the precise direction of the axis. This is what we mean by ‘recoil’.

Let us denote by  $\omega_s$  the energy of the soft wide-angle radiation that is neglected in the factorization (27). Neglecting this soft radiation in the determination of the jet axis will result in an axis  $\hat{n}_1(N_{J_c})$ , which differs from the axis  $\hat{n}_1(N)$  determined from the complete final state ( $N$ ) by an angle  $\Delta_s\phi$ :

$$\angle(\hat{n}_1(N), \hat{n}_1(N_{J_c})) \equiv \Delta_s\phi \sim \frac{\omega_s}{Q}. \quad (129)$$

At the same time, the soft, wide-angle radiation also contributes to the total event shape  $\bar{f}(N, a) \sim (1/Q)k_{\perp}^a(k^-)^{1-a}$  at the level of

$$\bar{\varepsilon}_s \sim \frac{\omega_s}{Q}, \quad (130)$$

because for such wide-angle radiation, we may take  $k_s^- \sim k_{s,\perp} \sim \omega_s$ . In summary, the neglect of wide-angle soft radiation rotates the jet axis by an angle that is of the order of the contribution of the same soft radiation to the event shape.

In the factorization (27), the contribution of each final-state particle is taken into account, just as in Eq. (21). The question we must answer is how the rotation of the jet axis affects these contributions, and hence the value of the event shape.

For a wide-angle particle, the rotation of the jet axis by an angle of order  $\Delta_s\phi$  in Eq. (129) leads to a negligible change in its contributions to the event shape, because its angle to the axis is a number of order unity, and the jet axis is rotated only by an angle of order  $\bar{\varepsilon}_s$ . Contributions from soft radiation are therefore stable under the approximation (23). The only source of large corrections is then associated with energetic jet radiation, because these particles are nearly collinear to the jet axis.

It is easy to see from the form of the shape function in terms of angles, Eq. (11), that for any value of parameter  $a$ , a particle of energy  $\omega_i$  at a small angle  $\theta_i$  to the jet axis  $\hat{n}_1(N)$  contributes to the event shape at the level

$$\bar{\varepsilon}_i \sim \frac{\omega_i}{Q} \theta_i^{2-a}. \quad (131)$$

The rotation of the jet axis by the angle  $\Delta_s\phi$  due to neglect of soft radiation may be as large as, or larger than,  $\theta_i$ . Assuming the latter, we find a shift in the  $\bar{\varepsilon}_i$  of order

$$\delta\bar{\varepsilon}_i \equiv \bar{\varepsilon}_i(\hat{n}_1(N)) - \bar{\varepsilon}_i(\hat{n}_1(N_{J_c})) \sim \frac{\omega_i}{Q} (\Delta_s\phi)^{2-a} \sim \frac{\omega_i}{Q} \left(\frac{\omega_s}{Q}\right)^{2-a} \sim \frac{\omega_i}{Q} \bar{\varepsilon}_s^{2-a}. \quad (132)$$

The change in  $\bar{\varepsilon}_i$  is thus suppressed by at least a factor  $\bar{\varepsilon}_s^{1-a}$  compared to  $\bar{\varepsilon}_s$ , which is the contribution of the wide-angle soft radiation to the event shape. The contributions of nearly-collinear, energetic radiation to the event shape thus change significantly under the replacement (23), but so long as  $a < 1$ , these contributions are power-suppressed in the value of the event shape, both before and after the approximation that leads to a rotation of the axis. For this reason, when  $a < 1$  (and only when  $a < 1$ ), the value of the event shape is stable whether or not we include soft radiation in the determination of the jet axes, up to corrections that are suppressed by a power of the event shape. In this case, the transition from Eq. (21) to Eq. (27) is justified.



## References

- [1] S. Bethke, in *Barcelona 1998, Radiative corrections: Application of quantum field theory to phenomenology*, p. 243, [hep-ex/9812026].  
CDF Collaboration and D0 Collaboration (Sally Seidel for the collaborations), *Jet physics at the Tevatron*, hep-ex/0205013.  
H1 Collaboration and ZEUS Collaboration (Oscar Gonzalez for the collaboration), *Jet physics at HERA*, hep-ex/0211063.
- [2] Yu. L. Dokshitzer, V. A. Khoze, S. I. Troyan, in *Perturbative quantum chromodynamics*, ed. A. H. Mueller (World Scientific, Singapore, 1989), p. 241.  
Yu. L. Dokshitzer, V. A. Khoze, S. I. Troyan, A. H. Mueller, *Rev. Mod. Phys.* **60**, 373 (1988).
- [3] H. Georgi, M. Machacek, *Phys. Rev. Lett.* **39**, 1237 (1977).  
C. L. Basham, L. S. Brown, S. D. Ellis, S. T. Love, *Phys. Rev. Lett.* **41**, 1585 (1978).  
A. De Rujula, J. R. Ellis, E.G. Floratos, M. K. Gaillard, *Nucl. Phys.* **B 138**, 387 (1978).  
G. C. Fox, S. Wolfram, *Phys. Rev. Lett.* **41**, 1581 (1978).  
G. Parisi, *Phys. Lett.* **B 74**, 65 (1978).  
J. F. Donoghue, F. E. Low, S.-Y. Pi, *Phys. Rev.* **D 20**, 2759 (1979).  
R. K. Ellis, D. A. Ross, A. E. Terrano, *Phys. Rev. Lett.* **45**, 1226 (1980).
- [4] E. Farhi, *Phys. Rev. Lett.* **39**, 1587 (1977).
- [5] G. Sterman, *Phys. Rev.* **D 19**, 3135 (1979).
- [6] S. Catani, G. Turnock, B. R. Webber, L. Trentadue, *Phys. Lett.* **B 263**, 491 (1991).  
S. Catani, L. Trentadue, G. Turnock, B. R. Webber, *Nucl. Phys.* **B 407**, 3 (1993).
- [7] S. Catani, G. Turnock, B. R. Webber, *Phys. Lett.* **B 295**, 269 (1992).
- [8] Yu. L. Dokshitzer, A. Lucenti, G. Marchesini, G. P. Salam, *JHEP* **9801**, 011 (1998) [hep-ph/9801324].
- [9] G. P. Korchemsky, G. Sterman, in *Moriond 1995: Hadronic:0383-392* [hep-ph/9505391];  
*Nucl. Phys.* **B 437**, 415 (1995) [hep-ph/9411211]; *Nucl. Phys.* **B 555**, 335 (1999) [hep-ph/9902341].  
Yu. L. Dokshitzer, B. R. Webber, *Phys. Lett.* **B 404**, 321 (1997) [hep-ph/9704298].  
A. V. Belitsky, G. P. Korchemsky, G. Sterman, *Phys. Lett.* **B 515**, 297 (2001) [hep-ph/0106308].  
E. Gardi, J. Rathsman, *Nucl. Phys.* **B 638**, 243 (2002) [hep-ph/0201019].
- [10] N. A. Sveshnikov, F. V. Tkachov, *Phys. Lett.* **B 382**, 403 (1996) [hep-ph/9512370].  
F.V. Tkachov, *Int. J. Mod. Phys.* **A 12**, 5411 (1997) [hep-ph/9601308].  
G. P. Korchemsky, G. Oderda, G. Sterman, in *5th International Workshop on Deep Inelastic*

- Scattering and QCD (DIS 97)*, AIP Conference Proceedings 407, ed. J. Repond, D. Krakauer (American Institute of Physics, Woodbury, NY 1978), p. 988, [hep-ph/9708346].  
C. F. Berger *et al.*, in *Proc. of the APS/DPF/DPB Summer Study on the Future of Particle Physics (Snowmass 2001)* ed. N. Graf, eConf **C010630**, P512 (2001) [hep-ph/0202207].
- [11] W. Bartel *et al.* [JADE Collaboration], Phys. Lett. **B 101**, 129 (1981); Z. Phys. **C 21**, 37 (1983).  
M. Althoff *et al.* [TASSO Collaboration], Z. Phys. **C 29**, 29 (1985).  
M. Z. Akrawy *et al.* [OPAL Collaboration], Phys. Lett. **B 261**, 334 (1991).  
R. Akers *et al.* [OPAL Collaboration], Z. Phys. **C 68**, 531 (1995).
- [12] J. R. Ellis, V. A. Khoze, W. J. Stirling, Z. Phys. **C75**, 287 (1997) [hep-ph/9608486].
- [13] B. Abbott *et al.* [D0 Collaboration], Phys. Lett. **B 464**, 145 (1999) [hep-ex/9908017].
- [14] N. Kidonakis, G. Oderda, G. Sterman, Nucl. Phys. **B 531**, 365 (1998) [hep-ph/9803241].
- [15] C. F. Berger, T. Kúcs, G. Sterman, Phys. Rev. **D 65**, 094031 (2002) [hep-ph/0110004].
- [16] J. Huston (CDF Collaboration), Int. J. Mod. Phys. **A16S1A**, 219 (2001).  
V. Tano, *The underlying event in hadron-hadron collisions*, hep-ex/0205023.
- [17] M. Dasgupta, G. P. Salam, Phys. Lett. **B 512**, 323 (2001) [hep-ph/0104277]; JHEP **0203**, 017 (2002) [hep-ph/0203009]; JHEP **0208**, 032 (2002) [hep-ph/0208073].
- [18] C. F. Berger, T. Kúcs, G. Sterman, *Interjet energy flow/event shape correlations*, hep-ph/0212343.
- [19] A. Banfi, G. Marchesini, Yu. L. Dokshitzer, G. Zanderighi, JHEP **0007**, 001 (2000) [hep-ph/0004027].  
S. J. Burby, N. Glover, JHEP **0104**, 029 (2001) [hep-ph/0101226].  
R. B. Appleby, M. H. Seymour, JHEP **0212**, 063 (2002) [hep-ph/0211426].
- [20] A. Banfi, G. Marchesini, G. Smye, JHEP **0208**, 006 (2002) [hep-ph/0206076].
- [21] J. C. Collins, D. E. Soper, Nucl. Phys. **B 193**, 381 (1981).
- [22] A. V. Manohar, M. B. Wise, Phys. Lett. **B 344**, 407 (1995) [hep-ph/9406392].
- [23] R. B. Appleby, M. H. Seymour, Ref. [19].
- [24] G. Sterman, Phys. Rev. **D 17**, 2773 (1978).
- [25] G. Sterman, in *QCD & Beyond*, proceedings of the Theoretical Advanced Study Institute in Elementary Particle Physics (TASI '95), ed. D.E. Soper (World Scientific, Singapore, 1996) [hep-ph/9606312].

- [26] J. C. Collins, D. E. Soper, G. Sterman, *Factorization of hard processes in QCD*, in *Perturbative Quantum Chromodynamics*, ed. A. H. Mueller (World Scientific, Singapore, 1989), p. 1.
- [27] J. C. Collins, D. E. Soper, Nucl. Phys. B **194**, 445 (1982).
- [28] N. Kidonakis, G. Sterman, Nucl. Phys. B **505**, 321 (1997) [hep-ph/9705234].  
N. Kidonakis, G. Oderda and G. Sterman, Nucl. Phys. B **525**, 299 (1998) [hep-ph/9801268].
- [29] J. C. Collins, G. Sterman, Nucl. Phys. B **185**, 172 (1981).
- [30] H. Contopanagos, E. Laenen, G. Sterman, Nucl. Phys. B **484**, 303 (1997) [hep-ph/9604313].
- [31] Y. L. Dokshitzer, G. Marchesini, JHEP **0303**, 040 (2003) [hep-ph/0303101].
- [32] G. Oderda, Phys. Rev. D **61**, 014004 (2000) [hep-ph/9903240].
- [33] A. Sen, Phys. Rev. D **24**, 3281 (1981).  
G. P. Korchemsky, A. V. Radyushkin, Nucl. Phys. B **283**, 342 (1987).
- [34] J. C. Collins, D. E. Soper, G. Sterman, Nucl. Phys. B **250**, 199 (1985).
- [35] A. Gonzalez-Arroyo, C. Lopez, F. J. Yndurain, Nucl. Phys. B **153**, 161 (1979).  
G. Curci, W. Furmanski, R. Petronzio, Nucl. Phys. B **175**, 27 (1980).  
E. G. Floratos, C. Kounnas, R. Lacaze, Nucl. Phys. B **192**, 417 (1981).  
J. Kodaira, L. Trentadue, Phys. Lett. B **112**, 66 (1982).
- [36] S. Catani, L. Trentadue, Nucl. Phys. B **353**, 183 (1991).
- [37] G. Sterman, Nucl. Phys. B **281**, 310 (1987).  
S. Catani, L. Trentadue, Nucl. Phys. B **327**, 323 (1989).
- [38] G. P. Korchemsky, Mod. Phys. Lett. A **4**, 1257 (1989).  
S. Albino, R. D. Ball, Phys. Lett. B **513**, 93 (2001) [hep-ph/0011133].  
C. F. Berger, Phys. Rev. D **66**, 116002 (2002) [hep-ph/0209107].